

# Improved Scheme Using Remotely Sensed Geomorphological Characteristics to Investigate Fold-River Interactions for Major Rivers

Kevin P. Woodbridge<sup>1</sup>, Saied Pirasteh<sup>2</sup> and Daniel R. Parsons<sup>1\*</sup>

<sup>1</sup>Geography and Environment, School of Social Sciences and Humanities, Loughborough University, Epinal Way, Loughborough, LE11 3TU, UK. Email: kevinpaulwoodbridge@gmail.com, k.p.woodbridge@lboro.ac.uk (K.P.W.); Email: d.parsons@lboro.ac.uk (D.R.P)

## \*Corresponding Author

Daniel R. Parsons, Geography and Environment, School of Social Sciences and Humanities, Loughborough University, Epinal Way, Loughborough, LE11 3TU, UK. Email: d.parsons@lboro.ac.uk

**Submitted:** 2025, Apr 22; **Accepted:** 2025, May 23; **Published:** 2025, May 26

<sup>2</sup>Institute of Artificial Intelligence, Shaoxing University, Shaoxing, 508 West Huancheng Road, Yuecheng District, Zhejiang Province, Postal Code 312000, China. Email: spirasteh71@gmail.com

**Citation:** Woodbridge, K. P., Pirasteh, S., Parsons, D. R. (2025). Improved Scheme Using Remotely Sensed Geomorphological Characteristics to Investigate Fold-River Interactions for Major Rivers. *J Water Res*, 3(2), 01-38.

## Abstract

There are frequently interactions between active folds and major rivers (mean annual water discharges  $> 70 \text{ m}^3\text{s}^{-1}$ ). The major river may incise across the fold, to produce a water gap across the fold, or a bevelling (or lateral planation) of the top of the fold. Alternatively, the major river may be defeated to produce a diversion of the river around the fold, with wind gaps forming across the fold in some cases, or ponding of the river behind the fold. Why a river incises or diverts is often unclear, though influential characteristics and processes have been identified. A new, improved scheme for investigating fold-river interactions has been devised — based on Woodbridge et al., *Remote Sens.* 2019, 11, 2037, though superseding this and described in full here for ease of use — involving a short description of the major river, climate, and structural geology, and 13 characteristics of river and fold geomorphology: (1) Channel width,  $w$ , (2) Channel-belt width,  $cbw$ , (3) Floodplain width,  $fpw$ , (4) Channel sinuosity,  $Sc$ , (5) Braiding index,  $BI$ , (6) General river course direction,  $RCD$ , (7) Distance from fold core to location of river crossing,  $C-RC$ , (8) Distance from fold core to river basin margin,  $C-BM$ , (9) Width of geological structure at location of river crossing,  $Wgs$ , (10) Estimate of erosion resistance of surface sediments/rocks and deeper sediments/rocks in fold,  $ERs$ ,  $ERd$ , (11) Maximum channel bank migration rate,  $RMax$ , (12) Transverse topographic symmetry of floodplain at location of river crossing,  $TSF$ , (13) Estimate of fold total uplift rate,  $TUR$ . These geomorphological characteristics should be readily determinable for nearly all major rivers using widely available satellite imagery and fine scale geological maps, except for No. 13,  $TUR$ , for which additional data sources are needed, and which can be considered as a supplementary characteristic [1]. This study demonstrates the improved scheme in full, using the example of the major rivers Karun, Dez and Karkheh (mean annual water discharges  $575 \text{ m}^3\text{s}^{-1}$ ,  $230 \text{ m}^3\text{s}^{-1}$  and  $165 \text{ m}^3\text{s}^{-1}$ , respectively) interacting with active folds in the foreland basin tectonic setting of lowland south-west Iran. For these three major rivers, it was found that geomorphological characteristics Nos. 2, 3, 4, 6, 7, 11 and 12 had statistically significant differences ( $p\text{-value} \leq 0.05$ ) between categories of river incision across a fold and river diversion around a fold. The findings suggest that, in cases of river incision across a fold, there may be a reduction in the lateral migration of the river at the fold axis to increase the vertical incision of the river, to keep pace with fold uplift. Since it is likely that different characteristics will be important for other major rivers interacting with other folds, this scheme should be used to investigate a variety of major rivers from across the globe. By comparing the same parameters for different major rivers, a better understanding of fold-river interactions should be achieved.

**Keywords:** Major River, Fold, Geomorphology, Interactions, Remote Sensing, Characteristics, Tectonics, Karun, Dez, Karkheh, Iran, Khuzestan

---

## 1. Introduction

Interactions between rivers and tectonics can be fascinating, though difficult to interpret. Principally, this is because rivers are inherently variable and complex, influenced by a wide range of both autogenic factors that include topography, hydrology and sedimentology, and allogenic factors that include structural geology and active tectonics, plus human activities, climate and relative sea-level (or base level) changes [2–10]. Disentangling the various internal and external factors and their influences on geomorphology can be challenging. However, for major rivers, with mean annual water discharges of  $70 \text{ m}^3\text{s}^{-1}$  or more, interacting with active folds over horizontal spatial scales of metres to tens of kilometres (river channel dimensions to fold dimensions), the difficulties are lessened, especially at locations upstream of coastal plain-valleys [11–14].

This is because for a single major river at such scales, climate and rates of sediment supply from the basin hinterland are likely to be similar, as climate zones typically extend over scales of hundreds of kilometres, and upstream of the extent of the backwater length (typically a distance of more than 150 km from the shoreline) the influences of relative sea-level changes are likely to be minimal [13,15,17,18,19]. Hence, at these river reach scales, the significant allogenic factors will be limited to tectonics and human activities, with prominent human impacts being limited to the last few millennia [14,20–22].

Major rivers frequently interact with active folds, particularly as transverse rivers in foreland basin systems, where folds oriented roughly parallel to the orogenic axis may form a succession of “obstacles” to river courses, particularly in the orogenic wedge and foredeep [23,24]. Conceptual models of the interactions between transverse rivers and growing folds have been constructed [23–29]. Such models indicate that where rates of river aggradation exceed rates of structural uplift associated with the fold, a river will flow without impedance across the fold and may bevel off the top of the emerging fold with little or no topographic relief developing [28,29]. Where a fold does develop a surface topographic expression, a river will either flow across the fold by maintaining basinward-dipping channel slopes across the fold, or it will be defeated by the growing fold.

To maintain a transverse course across a fold, a river needs sufficient stream powers to erode and incise into the crest and across the axis of the fold at a rate greater than the difference between the rates of structural uplift and the rates of river aggradation [23, 30]. Whilst the precise controls on river erosion are debated, due to factors such as bed armouring, it is likely that river erosion into bedrock and sediments will be increased with greater stream powers [31,32]. If the river is defeated, then it will be diverted around the fold by channel migrations or avulsions to flow through structural

low points, frequently flowing initially roughly parallel to the fold axis and thence around the nose of the fold. Alternatively, the river may be ponded in a basin upstream of the fold, though this is not a frequent occurrence with major rivers, due to their greater discharges and stream powers [23,26,28,33].

According to such conceptual models, the responses of rivers and major rivers should be fairly predictable. A river may incise across an active fold as a water gap (a river valley of a maintained river course) or it may be defeated by the fold and diverted to leave a wind gap (a dry valley of a previous river course), with the configuration of these water and wind gaps varying with a number of factors, such as the type of fold [23,28,34,35]. For instance, detachment folds would be expected to have a wind gap near the centre of the fold and a water gap near the propagating fold tip, whilst fault bend folds would be expected to have a number of wind gaps across the length of the fold, with the defeated rivers diverted parallel to the fold axis [34,35].

Whilst conceptually it is clear that a major river should incise across an active fold in some cases and divert around it in other cases, in practice it is often unclear as to how and why this occurs. For instance, there is a seemingly paradoxical tendency for a number of major rivers to transect many growing anticlines in the vicinity of their greatest structural and topographic relief [36–38]. By contrast, some rivers frequently cross a growing fold near to the laterally propagating tip or nose of the fold [28,39]. Alternatively, rivers may be diverted around the fold tips of laterally propagating anticlinal fold segments until these fold segments coalesce; after which the river may divert away from the coalesced fold to feed a longitudinal river or it may incise across the coalesced fold at the topographic low of the merger location [40].

These different responses are probably due to changes in the fold-river interactions with time and the variable and complex nature of river systems [9,14,41,42]. There may be different reaction, relaxation and recurrence times for events, multiple processes may act in combination to produce a specific phenomenon, different factors may result in similar effects, a river system may not adjust in a progressive and systematic fashion to modifications, and a river system may be dominated by autogenic processes and exhibit variability independent of external factors, due to systems of non-linearity or self-organised criticality [10,42–46]. Nevertheless, with such systems there may be characteristics of the river or the fold which act as thresholds which the river needs to cross for the dynamic equilibrium of river incision across an active fold to develop and be maintained [43]. The characteristics which may act as thresholds will probably include those associated with the main controlling variables for the persistence of an antecedent river across a growing fold, shown in Table 1.

Variable	Effect
Rate of sediment aggradation and rate of structural uplift	Lower rates of sediment aggradation and lower rates of structural uplift promote persistence of an antecedent river, due to less erosion of the fold hanging wall being required
Erosion resistance of rocks and sediments within fold	Lower erosion resistances (thick alluvial strata, poor cementation, and readily erodible bedrock) mean that lower stream powers are required, thus promoting persistence of an antecedent river
Water discharge of river	Higher water discharges and higher stream powers promote persistence of an antecedent river
Stream power, flow depth, channel width, channel water surface slope of river	Higher stream powers promote persistence of an antecedent river. Narrower channel widths and steeper channel water surface slopes promote persistence of the antecedent river, due to associated increased stream powers
Sediment load	Increased sediment load decreases proportion of stream power available for bed erosion, mantling of the bed with sediment precludes erosion of bed; thus, reduced sediment load may promote persistence of an antecedent river
Width of geological structure	Widening of a geological structure causes reduced channel water surface slopes and stream powers; thus, narrower geological structures promote persistence of an antecedent river
Transverse structures	Transverse structures, such as faults, provide zones of less erosion resistant rocks that cut across structures, exploited by antecedent rivers

**Table 1: The Main Controlling Variables for the Persistence of Antecedent Rivers Crossing Growing Folds (Modified from [23,26,29]).**

The influences of some of these controlling variables are quite intricate, particularly those associated with river hydrology and sediment load [32]. For instance, a river crossing a fold will produce aggradation upstream and downstream of the fold in a dynamic equilibrium, in which sufficient foreland-dipping channel slopes for producing erosive stream powers across the zone of greatest fold uplift are maintained [23,28,47,48]. If upstream or downstream aggradation is insufficient, as may be the case with reduced sediment load, then the river may be defeated and diverted around the fold [23,25]. If upstream aggradation is excessive, then the river may be defeated by producing slopes that promote channel migrations or avulsions to other upstream locations [28,39,49].

If downstream aggradation is excessive, then the river may also be defeated by reducing channel slopes to such an extent that stream powers are insufficient to maintain erosion into the fold and maintain transport away of the eroded material [48]. Nevertheless, Table 1 still provides an adequate foundation for differentiating between river incision across a fold and river diversion around a fold. Some of the controlling variables, such as stream power, flow depth, and sediment load, involve characteristics which need to be determined by fieldwork; whereas other controlling variables, such as width of geological structure, involve characteristics which can be determined relatively easily from remote sensing imagery and fine scale geological maps.

### **1.1. Aim of the Study – A Scheme for Investigating Fold-River Interactions Using Remote Sensing**

The aim of this study is to demonstrate a new, improved scheme

which uses a short description of the major river and 13 remotely sensed characteristics of river and fold geomorphology to investigate fold-river interactions. The short description of the major river should include river measurements (including mean annual discharge) and short descriptions of the river course, climate, and structural geology. All of the geomorphological characteristics should be readily determinable from remote sensing imagery and fine scale geological maps, except for geomorphological characteristic No. 13, for which additional data sources are needed, and which can be considered as a supplementary characteristic.

This use of remote sensing allows a large number of rivers to be investigated relatively easily, without recourse to expensive and time-consuming fieldwork. This study utilises the example of the major rivers Karun, Dez and Karkheh interacting with folds in lowland south-west Iran to show how to apply the scheme in practice. The scheme was initially published in *Remote Sens.* 2019, 11, 2037, but the new, modified and improved scheme in this new article *supersedes* this [1]. The new, improved scheme for investigating fold-river interactions is described in full in this new article for ease of use, so that users of the scheme need only consult this new article. It includes two completely changed geomorphological characteristics and an expansion of the introductory dataset to include folds interacting with the River Karkheh.

### **1.2. Selection of 13 Remotely Sensed Characteristics of River and Fold Geomorphology**

Remote sensing imagery and fine-scale geological maps have

---

the advantage of being widely available data sources which only need processing for interpretation, rather than detailed fieldwork, but have the drawback that certain parameters, such as sediment grain size, sediment load, flow velocity, and channel depth, cannot be measured accurately from them. A number of the controlling variables in Table 1 involve geomorphological characteristics which are readily determinable from remote sensing and fine scale geological and topographical maps, as are other significant geomorphological characteristics, such as channel width, that are associated with other conceptual models [23,26–29].

Also, previous detailed studies on interactions between specific major rivers and tectonics, particularly those of Jorgensen involving rivers in western U.S.A., Lavé and Avouac involving upland rivers in Nepal, and Woodbridge involving lowland rivers in south-west Iran, have identified useful characteristics determinable using remote sensing and geological maps in their investigations of such interactions [14,50–52]. All of these data sources were used to compile a suite of 13 useful geomorphological characteristics to be determined in investigations of fold-river interactions:

- (1) Channel width,  $w$
- (2) Channel-belt width,  $cbw$
- (3) Floodplain width,  $fpw$
- (4) Channel sinuosity,  $Sc$
- (5) Braiding index,  $BI$
- (6) General river course direction, RCD
- (7) Distance from fold core to location of river crossing, C-RC
- (8) Distance from fold core to river basin margin, C-BM
- (9) Width of geological structure at location of river crossing,  $Wgs$
- (10) Estimate of erosion resistance of surface sediments/rocks and deeper sediments/rocks in fold, ERs, ERd
- (11) Maximum channel bank migration rate, RMax
- (12) Transverse topographic symmetry of floodplain at location of river crossing, TSF
- (13) Estimate of fold total uplift rate, TUR

The scheme was initially published by Woodbridge et al., 2019, but the new, modified and improved scheme described in full here in this new article supersedes this [1]. In particular, it includes completely changed geomorphological characteristics Nos. 11 and 12 (RMax and TSF), which should be readily accessible from remote sensing data sources (unlike the geomorphological characteristics previously used).

Geomorphological characteristics Nos. 1, 2 and 3 ( $w$ ,  $cbw$  and  $fpw$ ) are now measured for river reaches immediately upstream of the fold, across the fold axis (or its projection), and immediately downstream of the fold. Also, the relative integer scales for geomorphological characteristics Nos. 10 and 13 (ERs, ERd and TUR) are standardised so that they run from 0 (Net subsidence for TUR) through 1 (Extremely low) to 9 (Extremely high).

Summarising, channel width should be a useful parameter since the conceptual model of Amos and Burbank and the studies of Lavé and Avouac in Nepal indicate that channel width may act

as a key characteristic of river responses, with channel narrowing to enhance incision rates apparently taking precedence over other changes for upland rivers crossing rapidly uplifting folds [26,28,51–53].

Channel-belt width and floodplain width should be useful parameters, since narrowing of the channel-belt and narrowing of the floodplain at the location of the fold axis will increase the proportion of stream power available for vertical erosion and thus promote the maintenance of a river incising across a fold. The study of Woodbridge demonstrated the importance of channel-belt width, with a narrow average channel-belt width of less than c. 2.7 km being hypothesised as a threshold needed for the rivers Karun and Dez to produce and maintain river incision across a fold in lowland south-west Iran [14].

Channel sinuosity and braiding index should both be useful parameters, since the study of Woodbridge found trends for both reduced sinuosity and braiding index for river reaches incising across a fold; though, as with the studies of Jorgensen in U.S.A [14,50]. and Zámolyi in Hungary, these trends did not always achieve statistical significance [54]. General river course direction should be a useful parameter, as the study of Woodbridge found a tendency for river incision across a fold to have a general river course direction orthogonal to the fold axis for the river reaches which crossed the fold, whereas river diversion had a general river course parallel to the fold axis upstream of the fold, followed by a change in river course bearing of about 20°–70° to flow around the fold [14].

Distance from the fold core to the location where the river crosses the fold axis, should be a useful discriminative parameter since, naturally, there is very strong tendency for river incision across a fold to occur between the fold core and the fold nose, and for river diversion to occur beyond the fold nose [14,21,55]. Distance from the fold core to the river basin margin, should be a useful parameter if the timing of initial fold-river interactions is important, as hypothesised by Woodbridge [14].

Where a river incises across a fold due to it initially encountering the fold as a small, emerging fold, the fold core location is likely to be within the margins of the drainage basin of the river crossing the fold axis; whereas where a river diverts around a fold due to it initially encountering the fold as a larger, more developed fold, the fold core location is likely to be beyond the margins the drainage basin of the river crossing the fold axis, or its projection [14,21].

Width of geological structure should be a useful parameter, since, as shown in Table 1, the conceptual model of Burbank indicates that narrow geological structures promote river incision across a fold by avoiding the reduced channel slopes, stream powers, and vertical erosion associated with widening geological structures [23]. The erosion resistances of sediments and rocks in a fold can be estimated from fine scale geological maps where details of the sediments and rock types are known, and should be useful parameters since the conceptual models of Burbank and Bufe

---

indicate that low erosion resistances promote river incision across a fold and river bevelling of the top of a fold [23,29].

Also, some studies, such as that on the meandering of the River Dniester by Yeromenko and Ivanov [56], have found that variations in erosion resistances of rocks and sediments were significant in influencing river responses; though other studies, such as those on rivers and growing folds in northern Alaska reviewed by Burbank have found that variations in erosion resistances were not [23]. Maximum channel bank migration rate over time intervals of about 20 – 40 years should be a useful parameter, since lateral migration rates have been found to be significant in studies of river incision across a fold and river lateral planation of the top of a fold [14,29].

Transverse topographic symmetry of the floodplain is likely to be a useful parameter, particularly since the symmetry of a channel-belt within a river floodplain is likely to be significant over yearly to decadal timescales [28,57,58]. River diversion may result in a channel-belt located more towards the edge of the floodplain, due to the effects of tectonic tilting associated with a growing fold, in a manner analogous to that found by Cox using the similar parameter of transverse topographic symmetry of the drainage basin, for rivers in the Mississippi Embayment, USA, interacting with Quaternary tilt-block tectonics [28,59].

To determine fold total uplift rate, additional data sources are needed, hence, it can be considered as a supplementary geomorphological characteristic. Fold total uplift rate is included in the scheme as it should be a useful parameter, since, in a number of conceptual models, low rates of structural uplift promote the maintenance of a river incising across a fold [23,25,28,29].

## 2. Summary of Methods

There are two main elements to the application of the scheme to a specific major river or river system, as summarised here.

### 2.1. Short Description of River

The short description of the river introduces the major river and the context of the fold-river interactions. It should include data on river length, drainage basin area, mean annual water discharge, seasonality of discharge, and major direct human impacts on the river, and a short description of the river course. It should also include short descriptions of the regional climate and structural geology, with some details of the tectonic setting and the types of faults and folds. The short description of the river can be supplemented by maps of the river system and structural geology.

### 2.2. Measurement of Geomorphological Characteristics Nos. 1 to 13

The measurement of the first 12 characteristics of river and fold geomorphology provides the main data for investigating different fold-river interactions. The only data sources needed to determine these 12 remotely sensed characteristics are: high-resolution remote sensing images, including two sets of such images separated by about 20 – 40 years, fine scale geological maps (preferably at 1:100,000 scale or finer), and maps of oil and gas fields and seismic

survey sections (in cases where there are sub-surface folds). Such widespread data sources should be available for most of the major rivers of the world.

For geomorphological characteristics Nos. 1 to 6 (channel width, channel-belt width, floodplain width, channel sinuosity, braiding index, and general river course direction), the measurements are made for river reaches immediately upstream of the fold, across the fold axis (or its projection), and immediately downstream of the fold. This is done so that changes in these characteristics associated with the fold can be more easily differentiated from changes due to the sub-division into river reaches and other variations. For characteristic No. 6, general river course direction, it is changes relative to the fold axis which are more indicative of changes associated with the fold.

Hence, measurements for this characteristic are also made relative to the fold axis, and there is an emphasis on changes in river course direction between river reaches immediately upstream of the fold, across the fold axis, and immediately downstream of the fold [14].

Characteristics Nos. 7 to 10 (distances from fold core to location of river crossing and river basin margin, width of geological structure, and estimate of erosion resistance of sediments/rocks) are mainly associated with the structural geology, rocks, and sediments of the fold. Hence, for these characteristics, the measurements are made relative to structures of the fold, especially the fold core, the fold axis, and the fold limbs.

Characteristic No. 11 (maximum channel bank migration rate) is dependent on how the river is sub-divided into river reaches, and differences in the nature and time interval between the two sets of high-resolution images. Hence, measurements for this characteristic are made for river reaches immediately upstream of the fold, across the fold axis (or its projection), and immediately downstream of the fold.

Characteristic No. 12 (transverse topographic symmetry of floodplain) is concerned with the influences of fold growth and tectonic tilting on the position of the channel-belt within the floodplain. These influences will be greatest where the river channel thalweg crosses the fold axis (or its projection), hence measurements of characteristic No. 12 are made at this location.

The measurement of the final geomorphological characteristic, No. 13 (estimate of fold total uplift rate) requires data sources relating to vertical Earth surface movements that may not be available for all major rivers worldwide, hence it may be considered as a supplementary geomorphological characteristic. These additional data sources could include displaced geomorphic surfaces e.g., repeated precision GPS surveys, and precise levelling e.g. [60,61]. Fold total uplift rate is mainly associated with the structural geology of the fold. Hence, the estimates or measurements for this characteristic are made for the crest of the fold relative to the surrounding region.

### 3. Details of Methods for the 13 Geomorphological Characteristics Using the Rivers Karun, Dez and Karkheh as an Example

To introduce and demonstrate the use of the new scheme of 13 geomorphological characteristics, it has been applied to the River Karun, River Dez and River Karkheh in lowland south-west Iran in the province of Khuzestan, as an example. As shown in Figures 1 and Figure 2, the major rivers Karun, Dez and Karkheh (mean annual water discharge  $575 \text{ m}^3\text{s}^{-1}$ ,  $230 \text{ m}^3\text{s}^{-1}$  and  $165 \text{ m}^3\text{s}^{-1}$ , respectively) flow from the Zagros orogen in the N and NE across the Upper and Lower Khuzestan Plains into the Mesopotamian-Persian Gulf Foreland Basin to the S and SW [62]. Some of their interactions with folds within the Upper and Lower Khuzestan Plains have been subjected to detailed investigations [14,21,55].

The data in these investigations was used to provide short descriptions of the rivers Karun, Dez and Karkheh, as given in Section 4.1. The data was also used to demonstrate the measurement of each of the 13 geomorphological characteristics, by using the example of the Sardarabad Anticline (SDA on Figure 2), located several km to the north-west of Band-e Qir (Figure 1), and its interactions with the River Dez (river incision across the fold) and the River Karun (Shuteyt branch) (river diversion around the fold).

The Sardarabad Anticline appears to be a doubly plunging, segmented, asymmetric detachment fold which is about 58 km long  $\times$  9 km wide, and which rises to more than 70 m above the surrounding plains. The fold axis is oriented roughly ESE-WNW, curving to SE-NW at the eastern end, where it apparently merges with a roughly N-S oriented oblique lateral ramp [14,63–66].

For determining geomorphological characteristics Nos. 1 to 12 for the rivers Karun, Dez and Karkheh, the remote sensing images used were 30 m resolution false-colour Landsat Enhanced Thematic Mapper Plus (ETM+) images with Band 4 (near-infrared, 750-900 nm) displayed red, Band 3 (red, 630-690 nm) displayed green, Band 2 (visible green, 525-605 nm) displayed blue, and pan-sharpened with pan-chromatic Band 8 [67].

The fine-scale geological maps used were mainly 1:100,000 scale geological maps, such as “Sheet 20824E Mulla Sani” of the Iranian Oil Operating Companies, IOOC [68]. The maps of oil and gas fields and seismic survey sections were from a variety of sources [69–72].

The Landsat ETM+ images and detailed surveys of the rivers undertaken by the Dez Ab Engineering Company from 1997–2000 were used to sub-divide the main river courses of the Karun, Dez and Karkheh from the vicinity of Gotvand, Dezful and Pay-e-Pol in the N and NE, to the Persian Gulf and Huwayzah Marshes in the S and SW, into a succession of straight-line river reaches. The average river reach length was 8.0 km, with an extreme range of 0.8 – 50.5 km. A river reach was defined as a length of river channel with a relatively homogeneous discharge and morphology [73].

Significant changes in general river course direction, river planform, and river morphology were used to demarcate the end of one reach and the start of the next. This sub-division into river reaches, whilst necessarily subjective, facilitated the measurement of characteristics associated with river reaches, such as channel sinuosity and general river course direction [14,21].

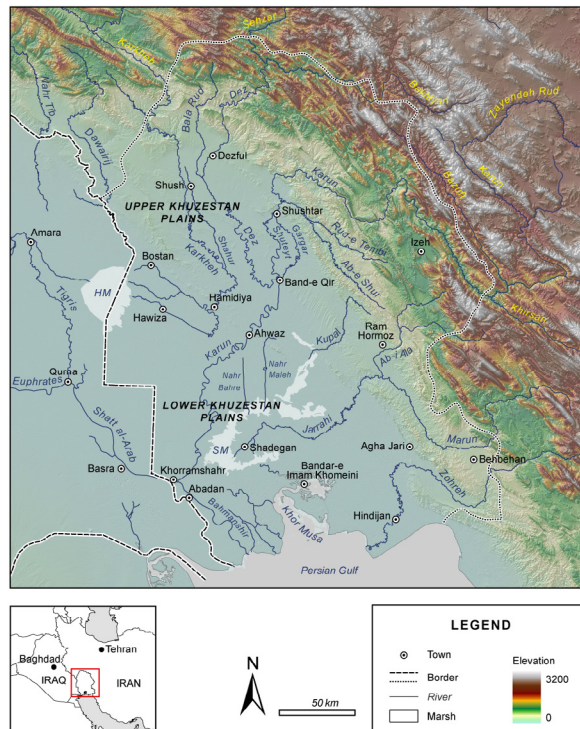


**Figure 1:** The River Karun, River Dez, River Karkheh and Other Main Rivers of Khuzestan Province and Its Environs (Modified from Heyvaert et al., 2013) [14,64]. Centred on  $31^{\circ}33'N$   $49^{\circ}02'E$ .

HM Huwayzah Marshes  
 ----- International border

SM Shadegan Marshes  
 ..... Border of Khuzestan province

The Sardarabad Anticline is a 58 km long by 9 km wide fold that is oriented roughly ESE-WNW and located to the north-west of the settlement of Band-e Qir (SDA on Figure 2).

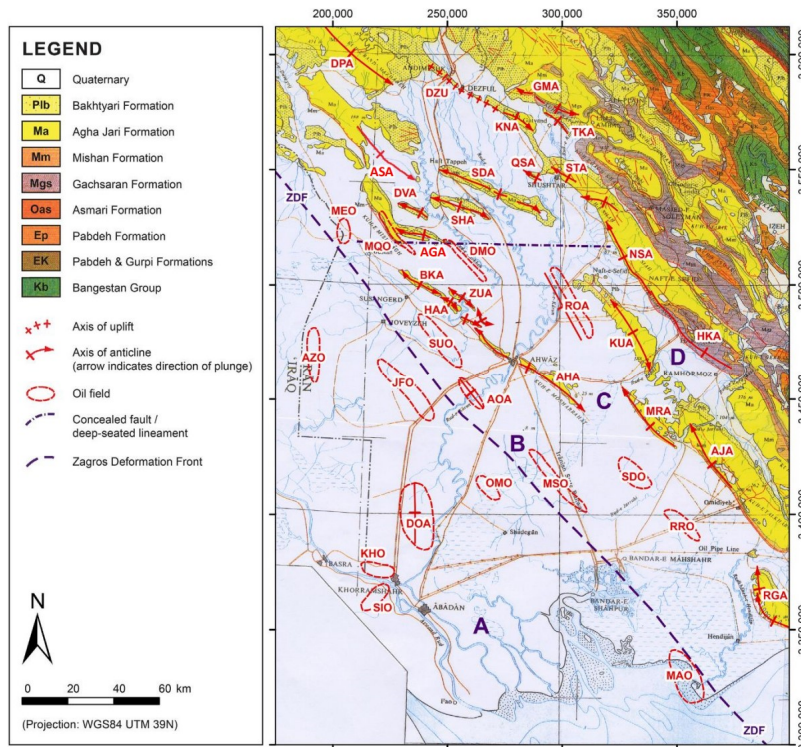


**Figure 2:** The Broad Scale Geology of South-West Iran, Showing Selected Anticlines, Oilfields and Oilfield Anticlines in the Lowlands (Modified from NIOC, 1973, using Various Sources) [14, 21, 65, 66]. Centred on 31°14'N 48°46'E. *Structural Geology:* AGA = Abu ul-Gharib Anticline, AHA = Ahvaz Anticline, AJA = Agha Jari Anticline, AOA = Ab-e Teymur Oilfield Anticline, ASA = Abu Salibi Anticline, AZO = Azadegan Oilfield, BKA = Band-e Karkheh Anticline, DMO = Dasht-e Mishan Oilfield, DOA = Dorquain Oilfield Anticline, DPA = Dal Parri Anticline, DVA = Darreh-ye Viza Anticline, DZU = Dezful Uplift, GMA = Gach-e Moh Anticline, HAA = Hamidiyyeh Anticline, HKA = Haft Kel Anticline, JFO = Jufeyr Oilfield, KHO = Khorramshahr Oilfield, KNA = Kuhanak Anticline, KUA = Kupal Anticline, MAO = Mahshahr Oilfield, MEO = Mehr Oilfield, MQO = Mushtaq Oilfield, MRA = Marun Anticline, MSO = Mansuri Oilfield, NSA = Naft-e Safid Anticline, OMO = Omid Oilfield, QSA = Qal'eh Surkkeh Anticline, RGA = Rag-e Safid Anticline, ROA = Ramin Oilfield Anticline, RRO = Ramshir Oilfield, SDA = Sardarabad Anticline, SDO = Shadegan Oilfield, SHA = Shahur Anticline, SIO = Siba Oilfield, STA = Shushtar Anticline, SUO = Susangerd Oilfield, TKA = Turkalaki Anticline, ZDF = Zagros Deformation Front (purple dashed line), ZUA = Zeyn ul-Abbas Anticline. *Geology:* Q = Quaternary (c. 1 Ma–Present; Generally Unconsolidated Alluvial Sands, Muds, Gravels, and Marls). Plb = Bakhtyari Formation (Middle Pliocene to Pleistocene, c. 3 Ma–1 Ma; Well-Consolidated Conglomerates, Sandstones, and Mudstones). Ma = Agha Jari Formation (Middle Miocene to Middle Pliocene, c. 10 Ma–3 Ma; Sandstones, Marls, and Mudstones). Mm = Mishan Formation (Middle Miocene, c. 16 Ma–10 Ma; Marls, Limestones, and Sandstones). Mgs = Gachsaran Formation (Early Miocene, c. 23 Ma–16 Ma; Anhydrite and Salt, Limestones, Marls, and Shales). Oas = Asmari Formation (Oligocene–Early Miocene; Mainly Limestones). Ep = Pabdeh Formation (Palaeocene–Oligocene; Mainly Marls and Shales). EK = Pabdeh & Gurpi Formations (Santonian–Oligocene; Mainly Marls and Shales). Kb = Bangestan Group (Late Cretaceous (Albian–Campanian); Mainly Limestones) [65–70]. *Approximate Zones of Earth Surface Movements:* A = Subsidence, B = Minimal Vertical Earth Surface Movements, C = Uplift at Rates of Approx 0.1–0.8 mm yr<sup>-1</sup>, D = Uplift at Rates of Approx 0.2–2.3 mm yr<sup>-1</sup> [14, 21, 55].

A superimposed database was constructed using false-colour Landsat ETM+ satellite images (dated 28 July and 4 August 2001), fine-scale geological maps, and CORONA satellite images (dated 23 September 1966 and 5 February 1968) which had been geo-referenced, orthorectified, and enhanced in a unified database using ArcGIS® software [74 – 76]. This database facilitated the

measurement of channel migrations with time, and facilitated easier measurement of characteristics associated with the fold core and fold axis.

For determining geomorphological characteristic No. 13, additional data relating to vertical Earth surface movements was used. This

data was of various types, including radiocarbon dating of marine terrace sediments and Optically Stimulated Luminescence (OSL) dating of river terrace sediments, and enabled estimates of fold total uplift rate to be made [14,21,55].

### 3.1. Channel Width

Symbol:  $w$

Units: m (quoted to two decimal places)

Measurement location: River reaches immediately upstream of fold, across the fold axis (or its projection), and immediately downstream of fold

Channel width is defined as the maximum extent of the river channel water surface, as distinguished on remote sensing images (or survey records), measured orthogonal to the river thalweg. Since the channel-forming discharge is commonly taken as the bankfull discharge and channel width varies significantly with river discharge, the aim is to measure the width between the channel banks at bankfull discharge [43,77]. In practice, channel width also varies with distance along the channel, local irregularities and outcrops, vegetation, human impacts, and other factors, so it is recommended that the distance between the channel banks is measured from remote sensing images of a single

date, preferably at a time of relatively high flows. Whilst variations could be reduced by determining average channel width over a distance of one or two meander wavelengths, subtle changes in channel width could be missed in the frequent cases where the zone of maximal uplift is considerably smaller than the meander wavelength of a major river [78,80]. Instead, for a single-thread meandering channel pattern, the width of the channel at, or very near to, the fold axis (or its projection) is measured, with care to avoid measuring at localised broadening or constriction of the channel. For a multi-thread braided channel pattern, the widths of all channels at the fold axis location are measured, and the sum recorded. For anastomosing or anabranching channel patterns, the widths of all channels associated with the main branch of the river at the fold axis location are measured, and the sum recorded [81]. Measurements are also made at, or very near to, the midpoint of the river reach immediately upstream of the fold and the midpoint of the river reach immediately downstream of the fold, to elucidate any changes in channel width associated with the fold.

For the example of the River Karun (Shuteyt) diverting around the Sardarabad Anticline, channel width,  $w = 202.19$  m, at the location where the projection of the fold axis intersects with the thalweg of the main river channel, as shown in Figure 3.

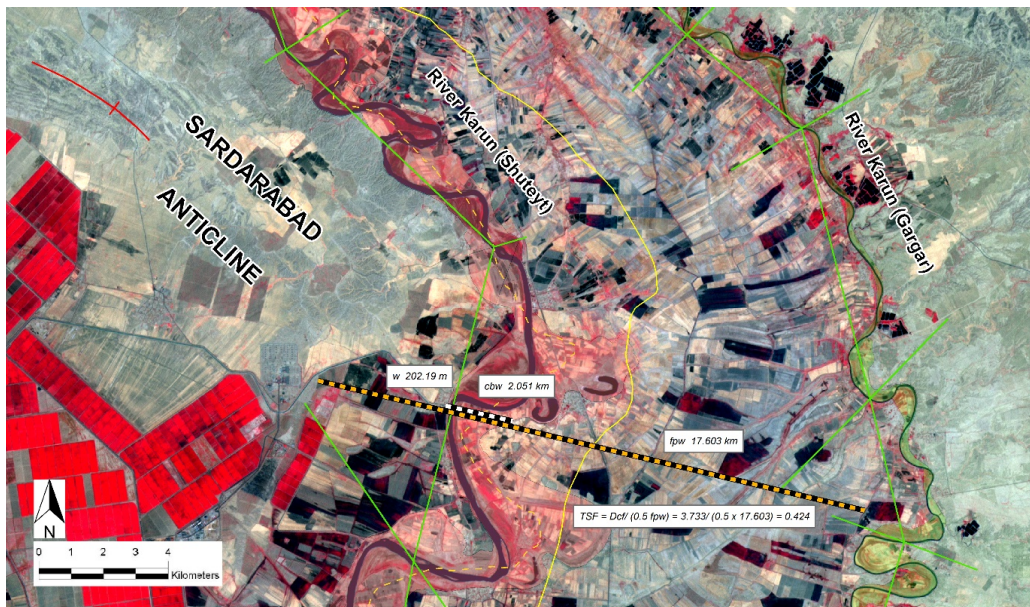


**Figure 3:** The Measurement of  $w$ ,  $cbw$ ,  $fpw$  and TSF (False-Colour Landsat Image (2001) of the River Karun (Shuteyt Branch) Diverting Around the Sardarabad Anticline, Centred on c.  $31^{\circ}52'N$   $48^{\circ}53'E$ ). Key: White and black Checked Straight Line =  $cbw$ , Light Brown and Black Checked Straight Line =  $fpw$ , Red Highlight = Channel-Belt of River Karun (Shuteyt), Green Highlight = Channel-Belt of River Gargar, Dashed Yellow Line = Channel-Belt Midline of River Karun (Shuteyt), Solid Yellow Line = Floodplain Midline of River Karun (Shuteyt), Red Line With Cross Bar = Axis of Anticline, Thin Green Line = Straight-Line River Reach (With Roughly Orthogonal Thin Green Lines Demarcating Successive Reaches).

### 3.2. Channel-Belt Width

Symbol:  $cbw$

Units: km (quoted to three decimal places)

Measurement location: River reaches immediately upstream of fold, across the fold axis (or its projection), and immediately downstream of fold

Channel-belt width is defined as the maximum extent of the channel-belt of the river, as distinguished on remote sensing images, measured orthogonal to the axis of the river reach. For single-thread meandering and straight channel patterns, the measurement is to the extremities of all channels, abandoned channels, meanders, levées, crevasse channels and splays, oxbows, and meander scars

that are associated with the active river channel. For a multi-thread braided channel pattern, the measurement is to the extremities of all channels, bars, islands, and abandoned channels associated with the active river channel [77]. For anastomosing or anabranching channel patterns, the measurement is to the extremities of the main active river channels, with any anabranches clearly separated by floodplain areas being considered as discrete channel-belts not included in the measurement [81]. Where there is uncertainty, such as discriminating between extensive braided rivers and discrete channels of anastomosing rivers, the default is to use the larger channel-belt width measurement. Measurements are made for river reaches immediately upstream of the fold, across the fold axis (or its projection), and immediately downstream of the fold, in the same manner as for geomorphological characteristic No. 1, to elucidate any changes in channel-belt width associated with the fold.

For the example of the River Karun (Shuteyt) diverting around the Sardarabad Anticline, channel-belt width,  $cbw = 2.051$  km, at the location where the projection of the fold axis intersects with the main river channel, as shown in Figure 3 by the white and black checked straight line.

### 3.3. Floodplain Width

Symbol:  $fpw$

Units: km (quoted to three decimal places)

Measurement location: River reaches immediately upstream of fold, across the fold axis (or its projection), and immediately downstream of fold

Floodplain width is defined as the maximum extent of the floodplain of the river, as distinguished on remote sensing images, measured orthogonal to the axis of the river valley. The floodplain width can vary from the channel-belt width to many tens of channel-belt widths [77]. The margins of the floodplain are usually fairly clear due to a slight change in slope at the base of the enclosing valley walls. Interpretive difficulties with floodplain width may arise where two or more major rivers occupy a large plain, especially a large coastal plain, and, in these cases, the measurement is to the extremities of the floodplain of the streams and wetlands within the drainage basin of the major river in question [82]. Measurements are made for river reaches immediately upstream of the fold, across the fold axis (or its projection), and immediately downstream of the fold, in the same manner as for geomorphological characteristic No. 1, to elucidate any changes in channel-belt width associated with the fold.

For the example of the River Karun (Shuteyt) diverting around the Sardarabad Anticline, floodplain width,  $fpw = 17.603$  km, at the location where the projection of the fold axis intersects with the main river channel, as shown in Figure 3 by the light brown and black checked straight line.

### 3.4. Channel Sinuosity

Symbol:  $Sc$

No units (ratio quoted to three decimal places)

Measurement location: River reaches immediately upstream of fold, across the fold axis (or its projection), and immediately downstream of fold

Channel sinuosity is the ratio defined by the equation:  $Sc = Lc/Lv$  where  $Lc$  is channel length (m), and  $Lv$  is straight-line valley length (m) [43]. The channel length is the total distance between the two ends of the river reach measured along the thalweg of the main channel. For multi-thread braided, anastomosing, and anabranching channel patterns there can be interpretive difficulties regarding the main channel thalweg, though, generally, it should be interpreted as the course of the broadest channel. The straight-line valley length is the distance between the two ends of the river reach measured in a straight line along the axis of the river reach.

For the example of the River Dez incising across the Sardarabad Anticline, channel sinuosity,  $Sc = 1.417$  (immediately upstream of fold); 1.120 (across fold axis); 1.585 (immediately downstream of fold), as shown in Figure 4.

### 3.5. Braiding Index

Symbol:  $BI$

No units (index quoted to one decimal place)

Measurement location: River reaches immediately upstream of fold, across the fold axis (or its projection), and immediately downstream of fold

The braiding index is a measure of the intensity of braiding, and for a river reach it can be defined as the channel count index of the mean number of anabranches (or links) per river cross-section for that reach, as described by Howard and Chew and Ashmore [83,84]. Since the intensity of braiding varies with flow stage, it is recommended that measurements are undertaken from remote sensing images of a single date, preferably at a time of relatively high flows for compatibility with other measurements, such as channel width [85]. The river reach is sub-divided into river cross-sections orthogonal to the valley axis which are approximately 1 km apart. For each river cross-section, the number of distinct anabranches is counted and the mean for the entire river reach is calculated. For single-thread meandering and straight channel patterns, the braiding index will be 1, or slightly greater than 1 where there are channel islands. For anastomosing or anabranching channel patterns, the braiding index is calculated for the main branch of the river.

For the example of the River Dez incising across the Sardarabad Anticline, braiding index,  $BI = 1.0$  (immediately upstream of fold); 1.2 (across fold axis); 1.2 (immediately downstream of fold), as shown in Figure 4.

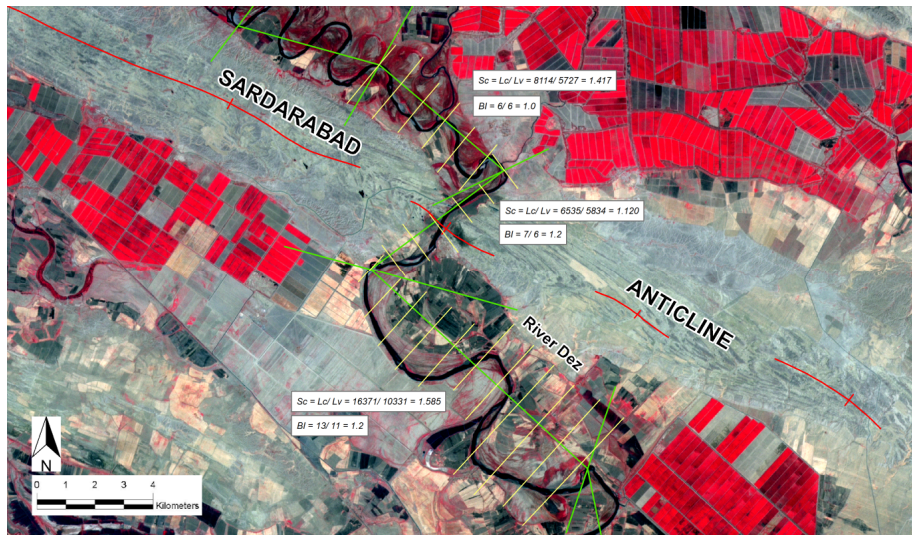


**Figure 4:** The measurement of  $Sc$  and  $BI$  (False-Colour Landsat Image (2001) of the River Dez Incising Across the Sardarabad Anticline, Centred on c.  $31^{\circ}57'N$   $48^{\circ}36'E$ ). Key: Thin yellow Line = Sub-Division of each River Reach into River Cross-Sections Orthogonal to the Valley Axis which are 1 km Apart, Red Line with Cross Bar = Axis of Anticline, Thin Green Line = Straight-Line River Reach (With Roughly Orthogonal Thin Green Lines Demarcating Successive Reaches).

### 3.6. General River Course Direction

Symbol: RCD

Units: degrees (quoted to the nearest  $5^{\circ}$ , as a compass bearing in degrees relative to true north, and as a bearing in degrees relative to the fold axis) Measurement location: River reaches immediately upstream of fold, across the fold axis (or its projection), and immediately downstream of fold.

The general river course direction is the general overall direction towards which the river flows for the length of a river reach [14]. This can be gauged “by eye” by carefully viewing the remote

sensing images and drawing a straight line of that orientation on the remote sensing image—the orientation of which will be similar to the river reach axes in the vicinity—and then measuring the bearing of that line to the nearest  $5^{\circ}$  to avoid false precision.

For the example of the River Dez incising across the Sardarabad Anticline, general river course direction,  $RCD = 130^{\circ}$  ( $10^{\circ}$  to fold axis) (immediately upstream of fold);  $230^{\circ}$  ( $70^{\circ}$  to fold axis) (across fold axis);  $135^{\circ}$  ( $15^{\circ}$  to fold axis) (immediately downstream of fold), as shown in Figure 5 by the white lines with black arrowheads.

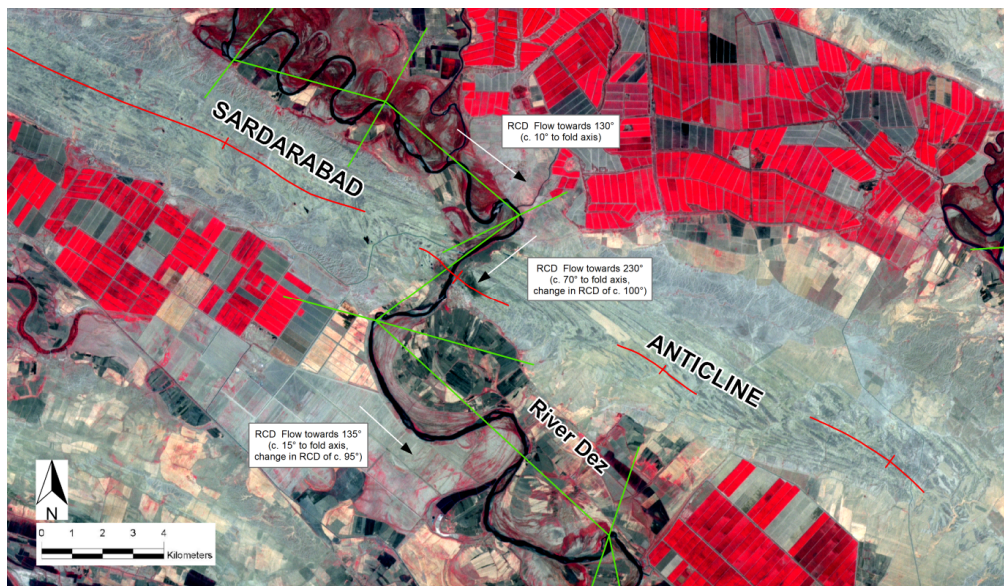


**Figure 5:** The measurement of RCD (False-Colour Landsat Image (2001) of the River Dez Incising Across the Sardarabad Anticline, Centred on c.  $31^{\circ}57'N$   $48^{\circ}37'E$ ). Key: White Line with Black Arrowhead = RCD, Red Line with Cross Bar = Axis of Anticline, Thin Green Line = Straight-Line River Reach (With Roughly Orthogonal Thin Green Lines Demarcating Successive Reaches).

### 3.7. Distance from Fold Core to Location of River Crossing

Symbol: C-RC

Units: km (quoted to one decimal place)

Measurement location: Along the fold axis, from the centre of the fold core to where the river channel crosses the fold axis (or its projection)

C-RC is defined as the horizontal distance from the centre of the fold core measured along the fold axis (and along the projection of the fold axis, where appropriate), to the location where the river channel thalweg crosses the fold axis or its projection [14]. This is most easily measured on fine scale geological maps (typically 1:100,000 or 1:50,000 scale geological maps, depending on availability) on which the surface lithology, structural geology (including the surface extent and anticlinal axis of each fold), and river channels are accurately shown.

The river crossing location is determined simply from where the fold axis (or its projection) intersects with the thalweg of the main river channel, as indicated on the fine scale geological map or on the remote sensing image. Where the main river channel has more than one intersection with the fold axis, as may be the case with a sinuous river, the intersection that is nearest to the fold core will be considered the river crossing location.

The location of the centre of the fold “core” (the centre of the main part of the fold which emerged first on the ground surface) is considerably more difficult to determine, since the detailed developmental history of a fold is usually not known. For ease of measurement, the centre of the fold core should be located on the fold axis. For sub-surface folds with little or no surface topographic expression, known principally from oil and gas field locations and seismic surveys, the centre of the fold core should be

interpreted as being midway along the approximate location of the fold axis on the ground surface (with particular consideration of the dip of sub-surface structures and stratigraphy).

This interpretation can be modified in cases where the sub-surface structural geology is well known. For young, emerging folds the centre of the fold core can be interpreted with more confidence and will usually be coincident with the centre of the surface topographic expression of the fold. For older, emerged folds the location of the centre of the fold core is much less certain. It can generally be interpreted to be in the vicinity of the structurally highest part of the present-day fold, which depending on the specific fold could be near its highest topographic expression, midway along the fold axis, or near to where it merges with an older, more developed fold [14,40,86].

For the example of the River Dez incising across the Sardarabad Anticline, distance from fold core to location of river crossing, C-RC = 1.3 km, as shown in Figure 6 by the solid dark green line with two black arrowheads. For the River Karun (Shuteyt) diverting around the Sardarabad Anticline, C-RC = 32.2 km, as shown in Figure 6 by the dashed dark green line with two black arrowheads.

In Figures 6 to 8: White = Quaternary Alluvium and Recent Deposits (c. 1 Ma–Present; generally unconsolidated alluvial sands, muds, gravels, and marls). Yellow (Bk) = Bakhtyari Formation (Middle Pliocene to Pleistocene, c. 3 Ma–1 Ma; well-consolidated conglomerates, sandstones, and mudstones). Dark orange (Aj) = Agha Jari Formation (Middle Miocene to Middle Pliocene, c. 10 Ma–3 Ma; sandstones, marls, and mudstones). Light orange (Lbm) = Lahbari Member of Agha Jari Formation (Early to Middle Pliocene, c. 5.5 Ma–3 Ma; mudstones, marls, and sandstones) [68,70,87,88].

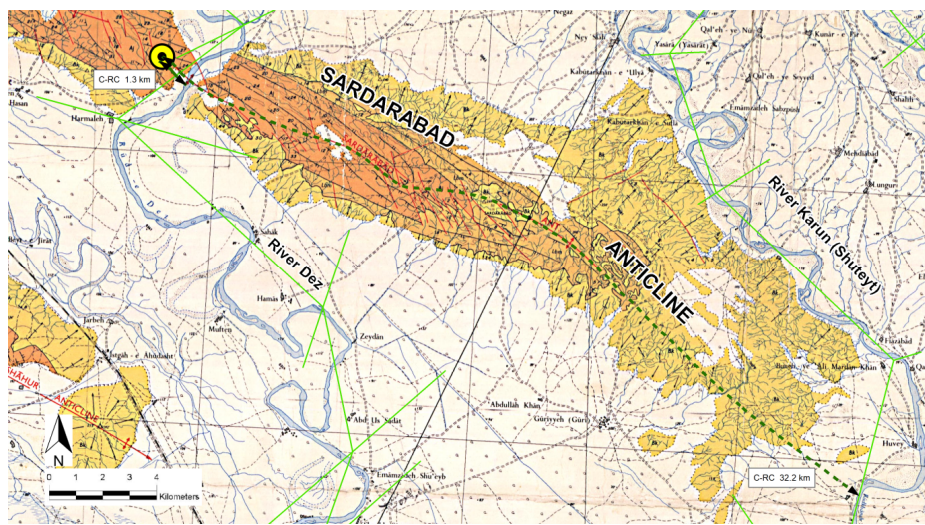


**Figure 6:** The Measurement of C-RC (Fine scale 1:100,000 Geological Map (IOOC, 1969 [68]) of the River Dez and River Karun (Shuteyt branch) Interacting with the Sardarabad Anticline, Centred on c. 31°54'N 48°42'E). Key: Solid Dark Green Line with Two Black Arrowheads = C-RC for River Dez, Dashed Dark Green Line with Two Black Arrowheads = CR-C for River Karun (Shuteyt), Black and Yellow Circle = Centre of Fold Core, Red line with Cross Bar = Axis of Anticline, Thin Green Line = Straight-Line River Reach (With Roughly Orthogonal Thin Green Lines Demarcating Successive Reaches).

### 3.8. Distance from Fold Core to River Basin Margin

Symbol: C-BM

Units: km (quoted to one decimal place, indicating +ve or -ve)

Measurement location: Along the fold axis, from the centre of the fold core to the nearest margin of the drainage basin of the river interacting with the fold.

C-BM is defined as the horizontal distance from the centre of the fold core, measured along the fold axis (and along the projection of the fold axis, where appropriate), to the nearest margin of the drainage basin of the river interacting with the fold [14]. The centre of the fold core is determined from fine scale geological maps, as described in Section 3.1.7.

The drainage basin margins are demarcated from remote sensing images or topographical maps, by determining which river

channels, wadis, lakes, streams, and creeks are associated with each major river and by drawing a line midway between the extents of these. The zero point for measurements is at the centre of the fold core, with +ve values where the fold core is located within the drainage basin of the river interacting with the fold, and -ve values where the fold core is located outside of the drainage basin of the river interacting with the fold.

For the example of the River Dez incising across the Sardarabad Anticline, distance from fold core to river basin margin, C-BM = +3.8 km, as shown in Figure 7 by the solid purple line with one black arrowhead. For the River Karun (Shuteyt) diverting around the Sardarabad Anticline, C-BM = -25.7 km, as shown in Figure 7 by the dashed purple line with one black arrowhead.

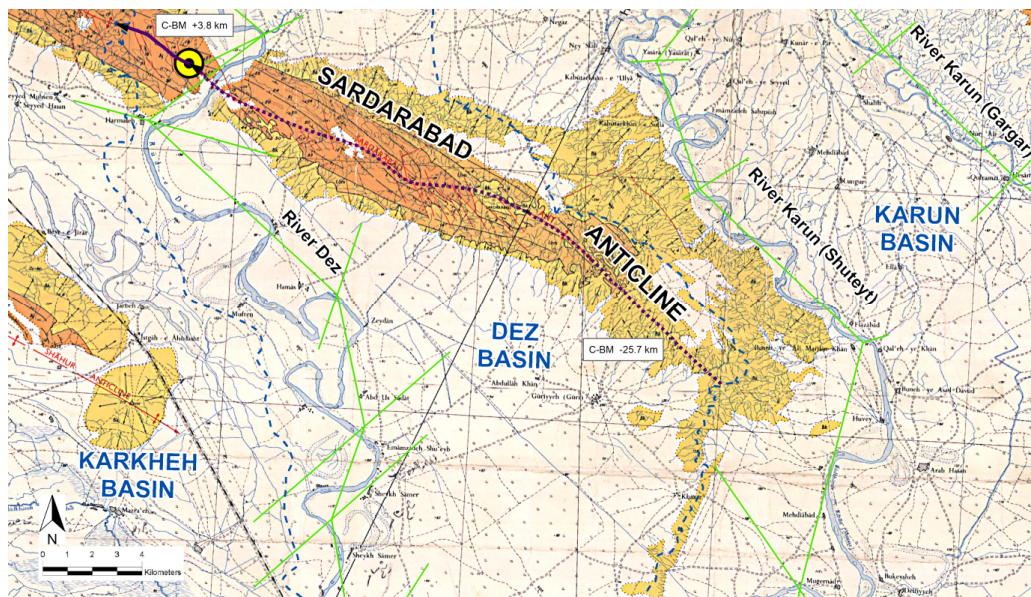


**Figure 7:** The Measurement of C-BM (Fine scale 1:100,000 Geological Map (IOOC, 1969 [67]) of the River Dez and River Karun (Shuteyt Branch) Interacting with the Sardarabad Anticline, Centred on c. 31°53'N 48°43'E). Key: Solid Purple Line with one Black Arrowhead = C-BM for River Dez, Dashed Purple Line with One Black Arrowhead = CR-C for River Karun (Shuteyt), Black and Yellow Circle = Centre of Fold Core, Blue Dashed Line = Drainage Basin Margin, Red Line with Cross Bar = Axis of Anticline, Thin Green Line = Straight-Line River Reach (With Roughly Orthogonal Thin Green Lines Demarcating Successive Reaches).

### 3.9. Width of Geological Structure at Location of River Crossing

Symbol: Wgs

Units: km (quoted to one decimal place)

Measurement location: Locality where river channel thalweg crosses the fold axis (or its projection)

Wgs is defined as the maximum horizontal surface extent of the geological structure at the location where the river channel thalweg crosses the fold axis (or its projection), measured orthogonal to the fold axis (or its projection) [14]. For sub-surface folds with little or no surface topographic expression, known principally from oil and gas field locations and seismic surveys, this measurement is necessarily approximate.

For river incision across a fold, the measurement is made orthogonal to the interpreted fold axis, between the margins of the mapped oil or gas field. For river diversion around a fold, the measurement is made orthogonal to the projection of the interpreted fold axis, between the projected margins of the nose of the mapped oil or gas field; a measurement which is highly subjective.

For emerged folds with significant surface topographic expression, this measurement is much more certain. For river incision across a fold, the measurement is made orthogonal to the fold axis, between the surface extent of the fold limbs as determined from fine scale geological maps and fine scale topography. For river diversion around a fold, the measurement is made orthogonal

to the projection of the fold axis, between the projected surface extent of the fold limbs of the nose of the fold; a measurement which is moderately subjective.

For the example of the River Dez incising across the Sardarabad Anticline, width of geological structure,  $W_{gs} = 4.3$  km, as shown in Figure 8 by the thick blue-grey line. For the River Karun (Shuteyt) diverting around the Sardarabad Anticline,  $W_{gs} = 4.1$  km, as shown on Figure 8 by the thick red line.

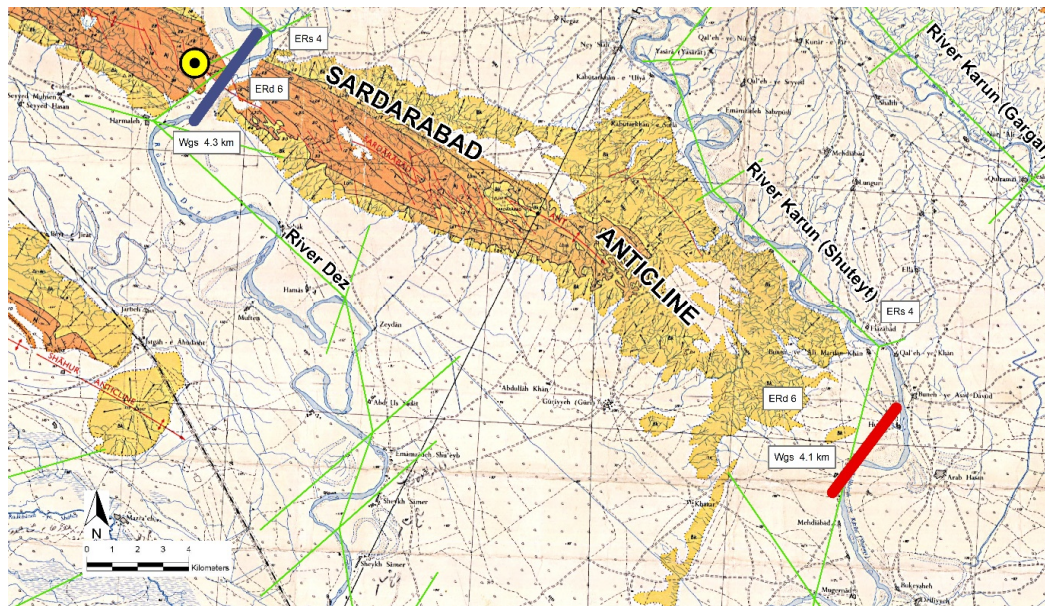


**Figure 8:** The Measurement of  $W_{gs}$ , ERs and ERd (Fine scale 1:100,000 Geological Map (IOOC, 1969 [67]) of the River Dez and River Karun (Shuteyt Branch) Interacting with the Sardarabad Anticline, Centred on c.  $31^{\circ}53'N$   $48^{\circ}43'E$ ). Key: Thick Blue-Grey Line =  $W_{gs}$  for River Dez, Thick Red Line =  $W_{gs}$  for River Karun (Shuteyt), Black and Yellow Circle = Centre of Fold Core, Red Line with Cross Bar = Axis of Anticline, Thin Green Line = Straight-Line River Reach (With Roughly Orthogonal Thin Green Lines Demarcating Successive Reaches).

### 3.10. Estimate of Erosion Resistance of Surface Sediments/Rocks and Deeper Sediments/Rocks in Fold

Symbols: ERs (surface); ERd (deeper)

No units (estimate quoted on a relative scale from 1 to 9)

Measurement location: Locality where the river channel thalweg crosses the fold axis (or its projection)

This characteristic is defined as the resistance of sediments and rocks in a fold to river erosion, a parameter which can be difficult to quantify. It depends upon a variety of characteristics including structural geology, rock type, sediment type, strength of intact rock (especially rock uniaxial compressive strength, rock tensile strength, rock mass strength, and rock mass deformation modulus), rock block volume, rock block shape and orientation relative to flow direction, internal stress and strain, resistance to weathering, jointing and fracturing (especially width, spacing, orientation, continuity and infilling of joints, and joint shear strength), degree of movement of water through the rock mass, moisture distribution, permeability, porosity, grain size, type and degree of cementation; as well as characteristics of the river, such as water discharge, nature and frequency of floods, river sediment supply, sediment discharge, suspended sediment concentration, and river bed roughness. Many of these characteristics are difficult to measure and their relative importance in determining the general erosion resistance of a fold is not fully known [23,32,74,89–96].

Hence, for each case an estimate of erosion resistance is made, and quoted as an integer on this scale:

1. Extremely low (Unlithified floodplain sediments – medium sands)
2. Very low (Unlithified floodplain sediments – predominantly sands).
3. Low (Unlithified floodplain sediments – predominantly muds)
4. Low/Moderate (Mainly unlithified floodplain sediments; some weathered and poorly consolidated bedrock, such as evaporites, mudstones, marls, poorly consolidated limestones like chalk, and poorly consolidated sandstones like those of the Agha Jari Formation bedrock).
5. Moderate (“Very weak rock” – crumbles with sharp blows from geological pick point; can be cut with penknife; uniaxial compressive strength c. 1–25 MPa; Schmidt Hammer N-type Rebound values c. 10–35 – mainly weathered and poorly consolidated bedrock, such as evaporites, mudstones, marls, poorly consolidated limestones like chalk, and poorly consolidated sandstones like those of the Agha Jari Formation bedrock; some unlithified floodplain sediments).
6. Moderate/High (“Weak rock” – deep indentation with firm blow from geological pick point, shallow cuts or scrapes can be made with penknife with difficulty; uniaxial compressive strength c. 25–50 MPa; Schmidt Hammer N-type Rebound values c. 35–40 – some poorly consolidated bedrock, such as coal and siltstones;

---

some well consolidated bedrock, such as well consolidated limestones, sandstones, shales, schists, and well consolidated conglomerates like those of the Bakhtyari Formation bedrock; few unlithified floodplain sediments).

7. High (“Moderately strong rock” – shallow indentation with firm blow from geological pick point; surface cannot be scraped or peeled with penknife; uniaxial compressive strength c. 50–100 MPa; Schmidt Hammer N-type Rebound values c. 40–50 – mainly well consolidated bedrock, such as well consolidated limestones, dolomites, marbles, sandstones, shales, slates, schists, and well consolidated conglomerates like those of the Bakhtyari Formation bedrock).

8. Very high (“Strong rock” – one firm blow from geological hammer breaks hand-held sample; uniaxial compressive strength c. 100–200 MPa; Schmidt Hammer N-type Rebound values c. 50–60 – very erosion resistant bedrock, such as well consolidated limestones and sandstones, metasandstones, marbles, basalts, granites, gabbros, gneisses, and other competent igneous and metamorphic rocks).

9. Extremely high (“Very strong rock” – many blows from geological pick required to break intact sample; uniaxial compressive strength c. >200 MPa; Schmidt Hammer N-type Rebound values c. >60 – extremely erosion resistant bedrock, such as quartzites, cherts, dolerites, basalts, granites, gabbros, gneisses, andesites, and other dense fine-grained igneous and metamorphic rocks) [97,98].

The position on this scale can be determined by careful interpretation of fine scale geological maps and remote sensing images, plus fieldwork and work on the properties of rocks and sediments, where available. The surface erosion resistance of the fold, ERs, is that of the surface lithology and sedimentology of the fold; especially that in the general vicinity of a river channel at the upstream location where the river first encounters the limb of the fold.

The deeper erosion resistance of the fold, ERd, is that of the deeper lithology and sedimentology of the fold; especially that exposed in the general vicinity of an incising river channel at the location of the fold axis. With emerging folds, ERd may be unknown in some cases where the sub-surface geology is only poorly known.

For the example of the River Dez incising across the Sardarabad Anticline, ERs = 4, ERd = 6, and for the River Karun (Shuteyt) diverting around the Sardarabad Anticline, ERs = 4, ERd = 6, as shown on Figure 8. For the location of the River Dez crossing, ERs = Low/Moderate (surface of unlithified floodplain sediments, with outcrops of Bakhtyari Formation bedrock (well consolidated conglomerates) and Agha Jari Formation bedrock (quite poorly cemented sandstones) at SW, W and E edges of floodplain), and ERd = Moderate/High (Bakhtyari Formation bedrock (well consolidated conglomerates) overlying Agha Jari Formation bedrock (quite poorly consolidated sandstones)). For the location of the River Karun (Shuteyt) crossing, ERs = Low/Moderate

(surface of unlithified floodplain sediments, with outcrops of Bakhtyari Formation bedrock (well consolidated conglomerates) at SW and W edges of floodplain), and ERd = Moderate/High (assuming Bakhtyari Formation bedrock overlying Agha Jari Formation bedrock).

### 3.11. Maximum Channel Bank Migration Rate

Symbol: RMax

Units: m yr<sup>-1</sup> (quoted to three decimal places)

Measurement location: River reaches immediately upstream of fold, across the fold axis (or its projection), and immediately downstream of fold

RMax, the maximum channel bank migration rate for a river reach over a specified period, can be defined by the equation:  $R_{Max} = B_{Max}/yr$  where BMax is maximum channel bank migration distance between corresponding points of a river bank on remote sensing images of different dates (m) and yr is number of years between remote sensing images. RMax is similar to migration rate, Rm, described by Giardino and Lee [99], though with the advantages of greater ease and simplicity of measurement, and less effects of smoothing of the data.

To determine RMax, the maximum channel bank migration rate, it is necessary to have access to high-resolution remote sensing images separated by a time interval of c. 20–40 years, and Geographic Information System (GIS) software (such as ArcGIS®) to orthorectify and superimpose the two sets of remote sensing images. Alternatively, accurate tracings of the river channel banks of one of the sets of high-resolution remote sensing images could be made, and superimposed on the other set. A time interval of c. 20–40 years should be long enough for significant channel migration to have taken place, though not so long that a channel may have migrated back to its original location.

Where possible, one set of images should be high resolution aerial photographs or satellite images from the 1960’s or earlier, so that the time interval includes periods prior to major dam building and other major human impacts. BMax for a river reach is determined by visually scanning along the channel banks of the superimposed remote sensing images of different dates, finding the location where there is the maximum separation of the two remote sensing images, and measuring the maximum straight-line distance between corresponding points (such as a meander apex or channel kink) on the two remote sensing images. BMax and RMax may be for the left bank or the right bank, the measurement used is the greatest measurement.

For the example of the River Dez incising across the Sardarabad Anticline, maximum channel bank migration rate, RMax = 51.907 m yr<sup>-1</sup> (immediately upstream of fold); 7.510 m yr<sup>-1</sup> (across fold axis); 27.671 (immediately downstream of fold), over a mean time interval of 34.2 years, as shown in Figure 9 by the yellow straight lines.

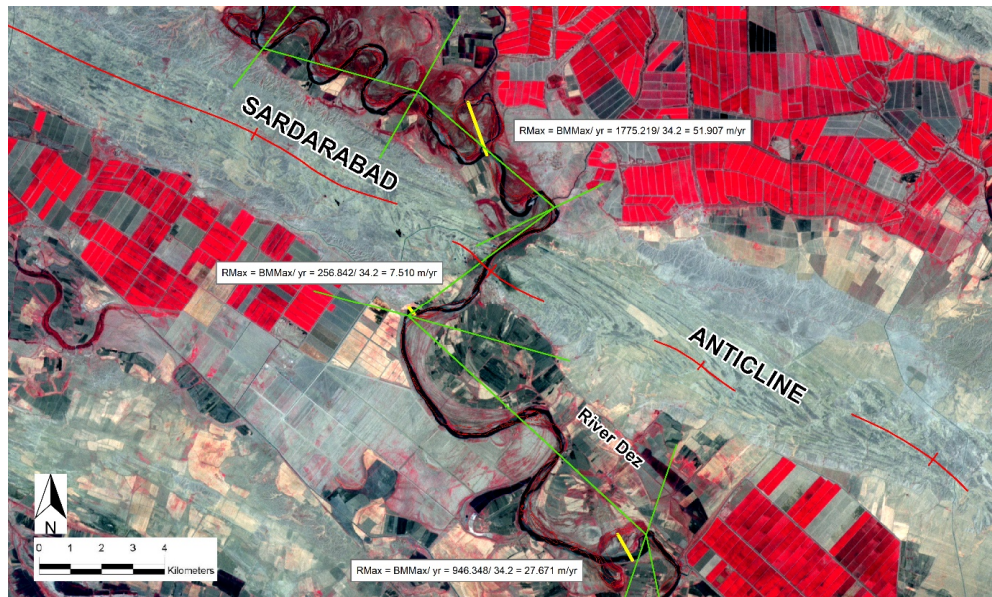


**Figure 9:** The Measurement of RMax (False-Colour Landsat Images (28 July and 4 August 2001) of the River Dez Incising Across the Sardarabad Anticline, Centred on c. 31°57'N 48°36'E). Key: Thin red lines = River Channel Banks on CORONA Satellite Images (23 September 1966 and 5 February 1968), Yellow Straight Line = RMax Over A Mean Time Interval of 34.2 Years, Red Line with Cross Bar = Axis of Anticline, Thin Green Line = Straight-Line River Reach (With Roughly Orthogonal Thin Green Lines Demarcating Successive Reaches).

### 3.12. Transverse Topographic Symmetry of Floodplain at Location of River Crossing

Symbol: TSF

Units: No units (ratio of symmetry, with 0.0 for channel-belt at centre of floodplain and 1.0 for channel-belt at edge of floodplain)  
Measurement location: Locality where river channel thalweg crosses the fold axis (or its projection).

Transverse topographic symmetry of the floodplain is the ratio defined by the equation:

$TSF = Dcf / Dmf = Dcf / (0.5 fpw)$  where  $Dcf$  is the distance from the channel-belt midline to the floodplain midline and  $Dmf$  (equivalent to  $0.5 fpw$  or half of the floodplain width) is the distance from the margin or edge of the floodplain to the floodplain midline. TSF is similar to transverse topographic symmetry,  $T$ , described by Cox (1994), though with TSF being concerned with the symmetry of the floodplain (rather than the symmetry of the drainage-basin), since the location of the channel-belt midline relative to the floodplain margin (rather than relative to the drainage divide) is more likely to be significant over the relatively short timescales of years and decades [28,59,57,58].

TSF is measured where the river channel thalweg crosses the fold axis (or its projection), a locality at which measurements of floodplain width,  $fpw$  and channel-belt width,  $cbw$  are also made. At this location, the position of the floodplain midline and  $0.5 fpw$  can be simply determined. Also at this location, the position of the measurement of  $cbw$  (be it for a meandering, braided, or anastomosing channel pattern) can be used to determine the position of the channel-belt midline and  $Dcf$ , the distance from the channel-belt midline to the floodplain midline. A record is made

of whether the channel-belt is displaced *towards* the fold core (that is, the channel-belt midline is nearer to the fold core than the floodplain midline), displaced *away from* the fold core (that is, the channel-belt midline is further away from the fold core than the floodplain midline), or central (with a TSF value of 0.01 or less).

For the example of the River Karun (Shuteyt) diverting around the Sardarabad Anticline, transverse topographic symmetry of floodplain at the location of the river crossing,  $TSF = Dcf / (0.5 fpw) = 3.733 / (0.5 \times 17.603) = 0.424$  ratio, towards the fold core, as shown in Figure 3.

### 3.13. Estimate of Fold Total Uplift Rate

Symbol: TUR

No units (estimate quoted on a relative scale from 0 to 9, roughly equivalent to ranges of rates of uplift in  $mm yr^{-1}$ )

Measurement location: At, or near to, the fold crest

The fold total uplift rate is defined as the rate at which a fold is rising above the surrounding region; that is, the single fold uplift rate less the sum of the regional subsidence rate and the sediment aggradation rate [30]. Generally, it is estimated or measured at, or near to, the fold crest because, in most cases, that is the part of the fold undergoing the greatest uplift relative to the surrounding region [100].

Fold total uplift rate cannot be determined solely from remote sensing images, remote sensing data, topographical maps, and geological maps. Other data sources are needed, which may be precision topographic survey (recurrent surveys over several

decades to determine vertical surface movements) e.g., or precision GPS survey (recurrent measurements from GPS stations over several years to determine horizontal and vertical surface movements) [61,101-104]. Alternatively, the data sources may be the measurement and dating of uplifted geomorphic markers, especially marine terraces and river terraces e.g, the measurement and dating of archaeological structures, especially disused ancient canals and the measurement and dating of structural geology, especially the development and erosion of fold growth strata e.g. [14,33,51,55,60,105-108].

Where such data is available for a fold, either by direct measurement or by careful interpretation, the estimated fold total uplift rate can be quoted as an integer on this relative scale:

0. Net subsidence (less than 0 mm yr<sup>-1</sup>, the fold uplift rate is less than the sum of the regional subsidence rate and the sediment aggradation rate)

1. Extremely low (about 0 – 0.05 mm yr<sup>-1</sup>)

2. Very low (about 0.05 – 0.1 mm yr<sup>-1</sup>)

3. Low (about 0.1– 0.2 mm yr<sup>-1</sup>)

4. Low/Moderate (about 0.2 – 0.5 mm yr<sup>-1</sup>)

5. Moderate (about 0.5 – 1.0 mm yr<sup>-1</sup>)

6. Moderate/High (about 1.0 – 2.0 mm yr<sup>-1</sup>)

7. High (about 2.0 – 5.0 mm yr<sup>-1</sup>)

8. Very high (about 5.0 – 10.0 mm yr<sup>-1</sup>)

9. Extremely high (more than 10.0 mm yr<sup>-1</sup>)

For the example of the River Dez incising across the Sardarabad Anticline, TUR = 4, and for the River Karun (Shuteyt) diverting around the Sardarabad Anticline, TUR = 4. The TUR for the Sardarabad Anticline was estimated to be Low/Moderate (about 0.2 – 0.5 mm yr<sup>-1</sup>) because OSL dating of river terrace sediments indicated uplift of the back-limb of the Sardarabad Anticline at a rate of 0.23–0.29 mm yr<sup>-1</sup> [14,21,55].

#### 4. Results of the New Scheme for the Rivers Karun, Dez and Karkheh

The results from applying the new, improved scheme to the River Karun, River Dez and River Karkheh interacting with folds and emerging folds in lowland south-west Iran are provided in Appendix A. This Appendix gives a short description of these rivers in Appendix A.1., followed by tables of the results for the 13 geomorphological characteristics in Tables 2–9 in Appendix A.2. It is recommended that a similar format is used when applying the scheme to other major rivers in different parts of the world. The findings of Analysis of Variance (ANOVA) between river incision across a fold and river diversion around a fold, applied to the 13 geomorphological characteristics for the rivers Karun and Dez, are given in Tables 10–11 in Appendix A.3. A discussion of these results is provided in Appendix B. The statistical significance of each of the 13 geomorphological characteristics for discriminating between river incision and river diversion for the rivers Karun, Dez and Karkheh are considered in Appendix B.1. and Appendix B.2.

## 5. Discussion

### 5.1. Interpretations of Fold-River Interactions for the Rivers Karun, Dez and Karkheh in Lowland South-West Iran

In cases of river incision across a fold, a narrow channel-belt and a narrow floodplain at the location of the fold axis are indicative of a reduction in the lateral migration of the river at the fold axis to increase the vertical incision of the river, to keep pace with fold uplift. The general scenario is one of broader channel-belts and floodplains immediately upstream and downstream of the fold due to increased aggradation to maintain channel slopes across the fold, and narrow channel-belts and floodplains across the fold due to increased erosion and incision, to keep pace with fold uplift [33,47,48]. As stated earlier, a narrow channel-belt is present in all cases of river incision, probably because a channel-belt is a relatively small feature that typically develops over time intervals of several decades or more, and a channel-belt width of 2.7 km or less may be a threshold for the rivers Karun, Dez and Karkheh in the Khuzestan Plains that needs to be maintained if a major river is incise across a fold in the long-term [14,57,58]. By contrast, a narrow floodplain is not present in all cases of river incision, probably because a floodplain is a significantly larger feature that typically develops over time intervals of centuries [64]. The strong tendency for a river to incise at locations near to the fold core, suggests that this river incision across a fold at, or near to, the fold core is initiated at a very early stage in fold development, probably when the fold is initially emerging on the ground surface [14].

These findings can help to explain the seemingly paradoxical tendency of rivers to transect both young and old anticlines at, or near to, locations of their greatest structural and topographic relief [36–38]. It can be considered that a fold initially emerges on the ground surface as a fold core, which in plan form may be an “oval”, a “sausage”, or another similar form, depending on the type of fold [34,86,138–140]. Where a major river initially encounters the fold as an emerging fold core, then the river may flow across the uplifting fold for sufficient time (at least several decades) for the development of a narrow channel-belt; thus, producing an incising river course across the fold in the vicinity of the fold core [57,58]. As the fold grows vertically and laterally, depending on the size and nature of the river, the incising river course may be maintained and become “fixed” to produce a water gap in the fold in the vicinity of the subsequent structural culmination, or the river may be subsequently defeated to produce a wind gap and a diverted river course [14,138]. By contrast, where a major river initially encounters a fold as a larger, emerged fold, the river may not flow across the uplifting fold for sufficient time for a narrow channel-belt to develop, due to repeated channel migration in response to lateral fold growth; thus, producing a river course diverting around the fold nose [14,21].

Interestingly, all of the geomorphological characteristics which are discriminatory at the 95 % confidence level, show trends which support this model. In cases of river incision across a fold, all of the trends and changes found are consistent with an increase in the erosion and vertical incision of the river at the location of the fold

axis, to keep pace with fold uplift. A reduction in mean channel sinuosity from 1.743 for the river reach immediately upstream of the fold to 1.208 for the river reach across the fold axis, will tend to increase the vertical incision of the river at the fold axis. This is because a shorter, straighter, river channel pattern is more erosive [43,77]. Similarly, a general river course direction that becomes more orthogonal to the fold axis for the river reach crossing the fold axis (mean value  $74.167^\circ$ ) and then reverts to the “original” river course direction for the river reach immediately downstream of the fold (mean value of change  $41.667^\circ$ ), will tend to increase the vertical incision of the river at the fold axis. This is because a shorter, more direct, river course is more erosive [43,77]. A reduced maximum channel bank migration rate at the fold axis (mean value of  $7.070 \text{ m yr}^{-1}$  for cases of river incision compared with a mean value of  $23.378 \text{ m yr}^{-1}$  for cases of river diversion), will tend to increase the vertical incision of the river across the fold axis. This is because a river with less lateral migration will have more stream power available for vertical erosion [28,43]. Similarly, a reduced transverse topographic symmetry of floodplain at the location where the river channel thalweg crosses the fold axis (TSF), will probably tend to increase the vertical incision of the river across the fold axis. This is because a river channel-belt located relatively near to the floodplain midline in cases of river incision, may be due to the river incising across a fold tending to incise relatively near to the fold “core” and then being less “mobile” (less subject to channel bank migration). A river with less lateral migration will have more stream power available for vertical erosion [28,43]. All of this indicates a strong influence of folds on the geomorphology of major rivers in the Khuzestan Plains.

## 5.2. Interpretations of Fold-River Interactions for Other Major Rivers

These observed changes apply for the major rivers Karun, Dez and Karkheh in lowland south-west Iran. To investigate whether similar or different changes apply with other major rivers and other folds, the scheme should now be applied to a variety of major rivers in a variety of environments from across the globe. For other fold-river interactions, it is likely that different changes will be found, and that other characteristics of river and fold geomorphology may discriminate between river incision across a fold and river diversion around a fold. Researchers may add other characteristics to the scheme as they see fit.

For instance, for the rivers Karun, Dez and Karkheh interacting with active folds in lowland south-west Iran, it was found that channel-belt width was a key discriminative characteristic, whereas channel width was not. By contrast, an investigation of two side-by-side upland rivers crossing rapidly uplifting folds (rates of uplift exceeding  $10 \text{ mm yr}^{-1}$ ) in the Himalayan foreland of central Nepal, found that both of the rivers exhibited a significant reduction in channel width across the zone of rock uplift [51,53,141]. The smaller Bakeya River became steeper across the zone of rapid uplift, whereas the larger Bagmati River showed no significant profile steepening across the same zone [51,52]. The research indicated that channel width acted as a key characteristic of river responses, and that if structural uplift should become sufficiently great, the

channel width would reduce to less than a certain threshold width value to maintain an incising river course across a zone of uplift. Channel narrowing to enhance incision rates appeared to take precedence over other changes, such as channel steepening and reduced river profile concavity; a scenario which has also been found with upland rivers elsewhere in the world [28,52,53]. In central Taiwan, in response to increasing rates of differential uplift, upland rivers in studies were found to have progressively narrower channel widths until a channel width:depth ratio of about 10 was reached, after which they also steepened [142]. In southern New Zealand, surveys of small upland channels indicated that 1 m–2 m of uplift resulted in a five- to ten-fold narrowing of river channels [26]. Such findings enabled Amos and Burbank to produce a conceptual model for a given river discharge, in which decreased channel width produced sufficient increased erosion to keep pace with uplift for small folds; whereas decreased channel width to a minimum value followed by subsequent channel steepening was needed to keep pace with uplift for larger folds [28]. Whilst these studies mainly involved smaller rivers, it is likely that there are significant differences between fold-river interactions in upland and lowland river catchments, with the geomorphological characteristic of channel width probably being more significant with upland rivers. This should be investigated by extending the database for the new scheme to a variety of upland rivers.

Also, it has been hypothesised that the seemingly paradoxical tendency for the major rivers Karun and Dez in lowland south-west Iran to transect anticlines near to locations of their greatest structural and topographic relief, is primarily due to the nature and timing of the initial fold-river interactions [14,21]. However, there are other mechanisms that may account for this, which apply after the initial stages of fold development. It may arise by the drainage network being superimposed from above via a structurally conformable more easily eroded horizon [36,37].

It may arise in areas where the crust is deforming plastically in response to regional compression, as a consequence of focussed rock uplift in response to significant differences between net erosion along major rivers and the surrounding regions, or in response to significant unloading of the crust by river erosion that amplifies the background deformation to produce a doubly plunging anticline with a river valley at its centre [94,143,144]. Alternatively, with continued crustal shortening and thickening, it may arise with amplification of a regional slope that produces higher erosion rates in transverse catchments than in longitudinal catchments, and which creates a new organisation of the drainage system following the regional slope [145].

It is likely that there will be notable differences in the relative significance of the geomorphological characteristics with each of these mechanisms, which should be investigated by extending the database for the scheme to a wide variety of major rivers in different tectonic settings from across the globe.

## 6. Conclusions

This study has demonstrated a new, improved scheme using remote

sensing for investigating fold-river interactions for major rivers. This scheme involved a short description of the major river, climate and structural geology, and 13 river and fold geomorphological characteristics. The scheme was initially published by Woodbridge et al., 2019, but the new, improved scheme described in full here in this new article *supersedes* this. In particular, it included completely changed geomorphological characteristics Nos. 11 and 12 (RMax and TSF), more readily accessible from remote sensing data sources, and an expansion of the introductory dataset that included folds interacting with the River Karkheh [1]. Researchers may add other characteristics to the scheme as they see fit.

The new, improved scheme for investigating fold-river interactions was successfully applied to the major rivers Karun, Dez and Karkheh in lowland south-west Iran. These rivers were similar, though sufficiently different to exhibit slightly different fold-river interactions, possibly related to their different discharges or catchment sizes [135]. Though the sample size was small, the River Karun (mean annual water discharge  $575 \text{ m}^3\text{s}^{-1}$ ) exhibited river incision in 80 % of cases, the River Dez ( $230 \text{ m}^3\text{s}^{-1}$ ) exhibited river incision in 67 % of cases, and the River Karkheh ( $165 \text{ m}^3\text{s}^{-1}$ ) exhibited river incision in 18 % of cases.

The scheme was found to be relatively easy to use in practice, mostly utilising data sources that were readily accessible, namely high-resolution remote sensing images (Landsat ETM+ and CORONA satellite images) and fine scale geological maps (IOOC 1:100,000 scale geological maps). For sub-surface folds, maps of oil and gas fields and seismic survey sections were utilised, involving time for a literature search to find data sources [69–72]. The main difficulty was with geomorphological characteristic No. 13, estimate of fold total uplift rate (TUR), for which additional data sources were needed which were quite difficult to access, variable in nature, and incomplete. Hence, since data for geomorphological characteristic No. 13 may not be available for all major rivers, it can be considered as a supplementary geomorphological characteristic.

For the major rivers Karun, Dez and Karkheh interacting with folds in lowland south-west Iran, it was found that seven geomorphological characteristics exhibited statistically significant differences at the 95 % confidence level ( $p\text{-value} \leq 0.05$ ) between categories of river incision across a fold and river diversion around a fold. These were: channel-belt width (cbw), floodplain width (fpw), channel sinuosity (Sc), general river course direction (RCD), distance from fold core to location of river crossing (C-RC), maximum channel bank migration rate (RMax), and transverse topographic symmetry of floodplain (TSF) (geomorphological characteristics Nos. 2, 3, 4, 6, 7, 11 and 12). The findings suggest that, in cases of river incision across a fold, there may be a reduction in the lateral migration of the river at the fold axis to increase the vertical incision of the river, to keep pace with fold uplift. Channel-belt width may be a key geomorphological characteristic, with a channel-belt width of 2.7 km or less probably being a threshold for the rivers Karun, Dez and Karkheh in the Khuzestan Plains that needs to be maintained if a major river is incised across a fold in the long-term [14].

The scenario in the foreland basin tectonic setting of lowland south-west Iran involves major rivers (of which the Karun, Dez and Karkheh are the largest) interacting with relatively young, emerging, thrust-related folds, with gradual earth surface movements predominating due to lubricated décollements on evaporite layers. The scheme should now be applied to a wide variety of major rivers of different sizes and discharges from different environments, climates, and tectonic settings from across the globe, to determine its usefulness in other scenarios and improve our knowledge of fold-river interactions. By comparing the same parameters for different major rivers, a better understanding of fold-river interactions should be achieved.

**Author Contributions:** Conceptualisation, K.P.W.; methodology, K.P.W., D.R.P., S.P.; software, K.P.W., S.P.; validation, S.P., K.P.W.; formal analysis, K.P.W.; investigation, K.P.W., S.P.; resources, K.P.W., D.R.P., S.P.; data curation, K.P.W., S.P., D.R.P.; writing—original draft preparation, K.P.W.; writing—review and editing, S.P., D.R.P.; visualisation, S.P., D.R.P., K.P.W.; supervision, D.R.P., S.P.; project administration, K.P.W., D.R.P., S.P.; funding acquisition, S.P., K.P.W., D.R.P.

**Acknowledgements:** Thanks, are expressed to the funding organisations for generous support, to the Geological Survey of Iran and the Khuzestan Water and Power Authority for collaborative fieldwork in south-west Iran, and to Prof. Mark Bateman and Dr. Morteza Fattahi at the SCIDR luminescence laboratory in Sheffield for associated OSL dating. Analysis of remote sensing images and maps of south-west Iran was undertaken with the kind assistance of the Geological Survey of Belgium, especially Prof. Vanessa Heyvaert and Dr. Jan Walstra.

**Conflicts of Interest:** The authors declare no conflict of interest.

**Submission Declaration and Verification:** This research work has been based on Woodbridge et al., *Remote Sens.* 2019, 11, 2037, but with modifications and improvements which supersede that previous publication [1]. The new, improved scheme for investigating fold-river interactions is described in full in this new article for ease of use, so that users of the scheme need only consult this new article.

**Data Availability:** All data are available upon request. Some data relating to the rivers Karun, Dez and Karkheh are provided in Appendices A and B.

## References

1. Woodbridge, K. P., Pirasteh, S., & Parsons, D. R. (2019). Investigating fold-river interactions for major rivers using a scheme of remotely sensed characteristics of river and fold geomorphology. *Remote Sensing*, 11(17), 2037.
2. Jones, S. J., Frostick, L. E., & Astin, T. R. (1999). Climatic and tectonic controls on fluvial incision and aggradation in the Spanish Pyrenees. *Journal of the Geological Society*, 156(4), 761-769.
3. Blum, M. D., & Törnqvist, T. E. (2000). Fluvial responses

- to climate and sea-level change: a review and look forward. *Sedimentology*, 47, 2-48.
4. Schumm, S. A., Dumont, J. F., & Holbrook, J. M. (2000). *Active tectonics and alluvial rivers* (Vol. 276). Cambridge: Cambridge University Press.
  5. Lang, A., Bork, H. R., Mäkel, R., Preston, N., Wunderlich, J., & Dikau, R. (2003). Changes in sediment flux and storage within a fluvial system: some examples from the Rhine catchment. *Hydrological Processes*, 17(16), 3321-3334.
  6. Vandenberghe, J. (2003). Climate forcing of fluvial system development: an evolution of ideas. *Quaternary Science Reviews*, 22(20), 2053-2060.
  7. Dollar, E. S. (2004). Fluvial geomorphology. *Progress in Physical Geography*, 28(3), 405-450.
  8. Brierley Gary, J., & Fryirs, K. A. (2005). *Geomorphology and River Management: Applications of the River Styles Framework*. Blackwell Publishing Company.
  9. Schumm, S. A. (2007). *River variability and complexity*. Cambridge University Press.
  10. Van De Wiel, M. J., & Coulthard, T. J. (2010). Self-organized criticality in river basins: Challenging sedimentary records of environmental change. *Geology*, 38(1), 87-90.
  11. Chapman, D. V. (2021). *Water quality assessments: a guide to the use of biota, sediments and water in environmental monitoring*. CRC Press.
  12. Nittrouer, J. A., Shaw, J., Lamb, M. P., & Mohrig, D. (2012). Spatial and temporal trends for water-flow velocity and bed-material sediment transport in the lower Mississippi River. *Bulletin*, 124(3-4), 400-414.
  13. Blum, M., Martin, J., Milliken, K., & Garvin, M. (2013). Paleovalley systems: insights from Quaternary analogs and experiments. *Earth-Science Reviews*, 116, 128-169.
  14. Woodbridge, K. P. (2013). *The influence of Earth surface movements and human activities on the River Karun in lowland south-west Iran* (Doctoral dissertation, University of Hull).
  15. Bryce, T. (1999). The Archaeology of Elam: Formation and Transformation of an Ancient Iranian State/DT Potts. *Prudentia*, 31(2), 160-162.
  16. Badripour, H., Suttie, J. M., & Reynolds, S. G. *Country Pasture/Forage Resource Profiles: Islamic Republic of Iran. 2006*.
  17. Peng, J., Chen, S., & Dong, P. (2010). Temporal variation of sediment load in the Yellow River basin, China, and its impacts on the lower reaches and the river delta. *Catena*, 83(2-3), 135-147.
  18. Shanley, K. W., & McCabe, P. J. (1992). Alluvial architecture in a sequence stratigraphic framework: a case history from the Upper Cretaceous of southern Utah, USA. *The geological modelling of hydrocarbon reservoirs and outcrop analogues*, 21-55.
  19. Li, C., Wang, P., Fan, D., & Yang, S. (2006). Characteristics and formation of Late Quaternary incised-valley-fill sequences in sediment-rich deltas and estuaries: case studies from China.
  20. Wilkinson, T. J. (2003). *Archaeological landscapes of the Near East*. University of Arizona Press.
  21. Woodbridge, K. P., Parsons, D. R., Heyvaert, V. M., Walstra, J., & Frostick, L. E. (2016). Characteristics of direct human impacts on the rivers Karun and Dez in lowland south-west Iran and their interactions with earth surface movements. *Quaternary International*, 392, 315-334.
  22. Alizadeh, A., Kouchoukos, N., Bauer, A. M., Wilkinson, T. J., & Mashkour, M. (2004). Human-environment interactions on the Upper Khuzestan Plains, southwest Iran. Recent investigations. *Paléorient*, 69-88.
  23. Burbank, D., Meigs, A., & Brozović, N. (1996). Interactions of growing folds and coeval depositional systems. *Basin research*, 8(3), 199-223.
  24. DeCelles, P. G., & Giles, K. A. (1996). Foreland basin systems. *Basin research*, 8(2), 105-123.
  25. Humphrey, N. F., & Konrad, S. K. (2000). River incision or diversion in response to bedrock uplift. *Geology*, 28(1), 43-46.
  26. Amos, C. B., & Burbank, D. W. (2007). Channel width response to differential uplift. *Journal of Geophysical Research: Earth Surface*, 112(F2).
  27. Douglass, J., Meek, N., Dorn, R. I., & Schmeckle, M. W. (2009). A criteria-based methodology for determining the mechanism of transverse drainage development, with application to the southwestern United States. *Geological Society of America Bulletin*, 121(3-4), 586-598.
  28. Burbank, D. W., & Anderson, R. S. (2013). Tectonic geomorphology.
  29. Bufe, A., Paola, C., & Burbank, D. W. (2016). Fluvial beveling of topography controlled by lateral channel mobility and uplift rate. *Nature Geoscience*, 9(9), 706-710.
  30. Doglioni, C., & Prosser, G. (1997). Fold uplift versus regional subsidence and sedimentation rate. *Marine and Petroleum Geology*, 14(2), 179-190.
  31. Sklar, L. S., & Dietrich, W. E. (2004). A mechanistic model for river incision into bedrock by saltating bed load. *Water Resources Research*, 40(6).
  32. Brocklehurst, S. H. (2010). Tectonics and geomorphology. *Progress in Physical Geography*, 34(3), 357-383.
  33. Burbank, D. W., & Beck, R. A. (1991). Rapid, long-term rates of denudation. *Geology*, 19(12), 1169-1172.
  34. Burberry, C. M., Cosgrove, J. W., & Liu, J. G. (2008). Spatial arrangement of fold types in the Zagros Simply Folded Belt, Iran, indicated by landform morphology and drainage pattern characteristics. *Journal of Maps*, 4(1), 417-430.
  35. Burberry, C. M., Cosgrove, J. W., & Liu, J. G. (2010). A study of fold characteristics and deformation style using the evolution of the land surface: Zagros Simply Folded Belt, Iran.
  36. Oberlander, T. M. (1965). The Zagros streams: a new interpretation of transverse drainage in an orogenic zone. *Syracuse geographical series*.
  37. Oberlander, T. M. (1985). Origin of drainage transverse to structures in orogens. In *Tectonic geomorphology* (Vol. 15, pp. 155-182). Allen and Unwin Boston.
  38. Alvarez. (1999). Drainage on evolving fold-thrust belts: A study of transverse canyons in the Apennines. *Basin*

- research, 11(3), 267-284.
39. Jackson, J., Norris, R., & Youngson, J. (1996). The structural evolution of active fault and fold systems in central Otago, New Zealand: evidence revealed by drainage patterns. *Journal of structural geology*, 18(2-3), 217-234.
  40. Ramsey, L. A., Walker, R. T., & Jackson, J. (2008). Fold evolution and drainage development in the Zagros mountains of Fars province, SE Iran. *Basin Research*, 20(1), 23-48.
  41. Downs, P., & Gregory, K. (2014). *River channel management: towards sustainable catchment hydrosystems*. Routledge.
  42. Schumm, S. A. (1998). *To interpret the earth: ten ways to be wrong*. Cambridge University Press.
  43. Knighton, D. (2014). *Fluvial forms and processes: a new perspective*. Routledge.
  44. Brunsdon, D., & Thornes, J. B. (1979). Landscape sensitivity and change. *Transactions of the Institute of British Geographers*, 463-484.
  45. Van De Wiel, M. J., Coulthard, T. J., Macklin, M. G., & Lewin, J. (2011). Modelling the response of river systems to environmental change: progress, problems and prospects for palaeo-environmental reconstructions. *Earth-Science Reviews*, 104(1-3), 167-185.
  46. Coulthard, T. J., & Van De Wiel, M. J. (2007). Quantifying fluvial non linearity and finding self organized criticality? Insights from simulations of river basin evolution. *Geomorphology*, 91(3-4), 216-235.
  47. Holbrook, J., & Schumm, S. A. (1999). Geomorphic and sedimentary response of rivers to tectonic deformation: a brief review and critique of a tool for recognizing subtle epeirogenic deformation in modern and ancient settings. *Tectonophysics*, 305(1-3), 287-306.
  48. Douglass, J., & Schmeckle, M. (2007). Analogue modeling of transverse drainage mechanisms. *Geomorphology*, 84(1-2), 22-43.
  49. Brozovic, N., Burbank, D. W., Fielding, E., & Meigs, A. J. (1995). The spatial and temporal topographic evolution of Wheeler Ridge California: new insights from digital elevation data. In *Geological Society of America Abstracts with Programs* (Vol. 27, No. 6, p. 396).
  50. Jorgensen, D. W. (1990). *Adjustment of alluvial river morphology and process to localized active tectonics*. Colorado State University.
  51. Lavé, J., & Avouac, J. P. (2000). Active folding of fluvial terraces across the Siwaliks Hills, Himalayas of central Nepal. *Journal of Geophysical Research: Solid Earth*, 105(B3), 5735-5770.
  52. Lavé, J., & Avouac, J. P. (2001). Fluvial incision and tectonic uplift across the Himalayas of central Nepal. *Journal of Geophysical Research: Solid Earth*, 106(B11), 26561-26591.
  53. Kirby, E., & Whipple, K. (2001). Quantifying differential rock-uplift rates via stream profile analysis. *Geology*, 29(5), 415-418.
  54. Zamolyi, A., Székely, B., Draganits, E., & Timár, G. (2010). Neotectonic control on river sinuosity at the western margin of the Little Hungarian Plain. *Geomorphology*, 122(3-4), 231-243.
  55. Woodbridge, K. P., & Frostick, L. E. (2014). OSL dating of Karun river terrace sediments and rates of tectonic uplift in lowland south-west Iran. *Quaternary Newsletter*, 134(4).
  56. YEROMENKO, V., & YA, E. V. (1977). STUDY OF RIVER MEANDERING IN THE SEARCH FOR TECTONIC STRUCTURES (ASEXEMPLIFIED BY THE MIDDLE DNIESTER REGION).
  57. Lahiri, S. K., & Sinha, R. (2012). Tectonic controls on the morphodynamics of the Brahmaputra River system in the upper Assam valley, India. *Geomorphology*, 169, 74-85.
  58. Geomorphic, P. (2004). Belt width delineation procedures. *Submitted to the Toronto and Region Conservation Authority*.
  59. Cox, R. T. (1994). Analysis of drainage-basin symmetry as a rapid technique to identify areas of possible Quaternary tilt-block tectonics: an example from the Mississippi Embayment. *Geological society of america bulletin*, 106(5), 571-581.
  60. Oveisi, B., Lavé, J., Van Der Beek, P., Carcaillet, J., Benedetti, L., & Aubourg, C. (2009). Thick-and thin-skinned deformation rates in the central Zagros simple folded zone (Iran) indicated by displacement of geomorphic surfaces. *Geophysical Journal International*, 176(2), 627-654.
  61. Ching, K. E., Hsieh, M. L., Johnson, K. M., Chen, K. H., Rau, R. J., & Yang, M. (2011). Modern vertical deformation rates and mountain building in Taiwan from precise leveling and continuous GPS observations, 2000–2008. *Journal of Geophysical Research: Solid Earth*, 116(B8).
  62. Pirasteh, S., Woodbridge, K., & Rizvi, S. M. A. (2009). Geo-information technology (GiT) and tectonic signatures: the River Karun & Dez, Zagros Orogen in south-west Iran. *International Journal of Remote Sensing*, 30(2), 389-403.
  63. Allen, M. B., & Talebian, M. (2011). Structural variation along the Zagros and the nature of the Dezful Embayment. *Geological magazine*, 148(5-6), 911-924.
  64. Heyvaert, V. M. A., Verkinderen, P., & Walstra, J. (2013). Geoaerchaeological research in Lower Khuzestan: state of the art. *Susa and Elam. Archaeological, Philological, Historical and Geographical Perspectives*, 493-534.
  65. National Iranian Oil Company (NIOC). *Geological Map of Iran Sheet No. 4 South-West Iran, 1: 1,000,000 Scale. (Including South-West Iran and Northern Persian Gulf Oil Fields); NIOC: Tehran, Iran, 1973*.
  66. National Iranian Oil Company (NIOC). *Tectonic Map of South-West Iran, 1: 2,500,000 Scale; NIOC: Tehran, Iran, 1977*.
  67. National Aeronautics and Space Administration (NASA). *About Landsat: Enhanced Thematic Mapper Plus*. 2012.
  68. Iranian Oil Operating Companies (IOOC). *Geological Compilation Map, 1:100000 Scale, Sheet No. 20824 E, Mulla Sani; IOOC, Geological and Exploration Division: Tehran, Iran, 1969*.
  69. Sherhati, S., & Letouzey, J. (2004). Variation of structural style and basin evolution in the central Zagros (Izeh zone and Dezful Embayment), Iran. *Marine and petroleum geology*, 21(5), 535-554.

70. Fard, I. A., Braathen, A., Mokhtari, M., & Alavi, S. A. (2006). Interaction of the Zagros Fold–Thrust Belt and the Arabian-type, deep-seated folds in the Abadan Plain and the Dezful Embayment, SW Iran. *Petroleum Geoscience*, 12(4), 347-362.
71. Maleki, M. E. H. R. D. A. D., Javaherian, A., & Abdollahi Fard, I. (2006). High porosity anomaly with good reservoir properties in the lower Fahliyan formation (Neocomian) of Darquain Field (SW Iran) by 3D seismic. *Journal of the Earth and Space physics*, 32(3), 33-39.
72. Soleimani, B., Nazari, K., Bakhtiar, H. A., Haghparast, G., & Zandkarimi, G. (2008). Three-dimensional geostatistical modeling of oil reservoirs: a case study from the ramin oil field in Iran. *Journal of Applied Sciences*, 8(24), 4523-4532.
73. Hogan, D. L., & Luzi, D. S. (2010). Channel geomorphology: fluvial forms, processes, and forest management effects. *Compendium of forest hydrology and geomorphology in British Columbia*, 1, 331-372.
74. Ali, S. A., & Pirasteh, S. (2004). Geological application of Landsat ETM for mapping structural geology and interpretation: aided by remote sensing and GIS. *Int J Remote Sens*, 25(21), 4715-4727.
75. Walstra, J., Heyvaert, V. M. A., & Verkinderen, P. submitted, Mapping the alluvial landscapes of Lower Khuzestan (SW Iran). *Geomorphological mapping: a professional handbook of techniques and applications*, Elsevier, Amsterdam.
76. Walstra, J., Verkinderen, P., & Heyvaert, V. M. (2010). 11. Reconstructing landscape evolution in the Lower Khuzestan plain (SW Iran): integrating imagery. *Landscapes Through the Lens: Aerial Photographs and the Historic Environment*, 111.
77. Bridge, J. S. (2009). *Rivers and floodplains: forms, processes, and sedimentary record*. John Wiley & Sons.
78. Rogerson, P. A. (2019). Statistical methods for geography: a student's guide.
79. Rosgen, D. L. (1994). A classification of natural rivers. *Catena*, 22(3), 169-199.
80. Bjerklie, D. M., Moller, D., Smith, L. C., & Dingman, S. L. (2005). Estimating discharge in rivers using remotely sensed hydraulic information. *Journal of hydrology*, 309(1-4), 191-209.
81. Makaske, B. (2001). Anastomosing rivers: a review of their classification, origin and sedimentary products. *Earth-Science Reviews*, 53(3-4), 149-196.
82. Nanson, G. C., & Croke, J. C. (1992). A genetic classification of floodplains. *Geomorphology*, 4(6), 459-486.
83. Howard, A. D., Keetch, M. E., & Vincent, C. L. (1970). Topological and geometrical properties of braided streams. *Water Resources Research*, 6(6), 1674-1688.
84. Chew, L. C., & Ashmore, P. E. (2001). Channel adjustment and a test of rational regime theory in a proglacial braided stream. *Geomorphology*, 37(1-2), 43-63.
85. Egozi, R., & Ashmore, P. (2008). Defining and measuring braiding intensity. *Earth surface processes and landforms*, 33(14), 2121-2138.
86. Bretis, B., Bartl, N., & Grasemann, B. (2011). Lateral fold growth and linkage in the Zagros fold and thrust belt (Kurdistan, NE Iraq). *Basin Research*, 23(6), 615-630.
87. James, G. A., & Wynd, J. G. (1965). Stratigraphic nomenclature of Iranian oil consortium agreement area. *AAPG bulletin*, 49(12), 2182-2245.
88. Hamzepour, B., Paul, D. J., & Wiesner, E. K. (1999). Views on the structural development of the Zagros simply folded Belt in Khuzestan Province, Iran. (10 fig.). *ZEITSCHRIFT-DEUTSCHEN GEOLOGISCHEN GESELLSCHAFT*, 150, 167-188.
89. Selby, M. J. (1980). A rock mass strength classification for geomorphic purpose: with tests from Antarctica and New Zealand. *Zeit. Geomorph.*, NF, 24, 31-51.
90. Ali, S. A., Rangzan, K., & Pirasteh, S. (2003). Remote sensing and GIS study of tectonics and net erosion rates in the Zagros structural belt, Southwestern Iran. *Mapping Sciences and Remote Sensing*, 40(4), 258-267.
91. VanLaningham, S., Meigs, A., & Goldfinger, C. (2006). The effects of rock uplift and rock resistance on river morphology in a subduction zone forearc, Oregon, USA. *Earth Surface Processes and Landforms: The Journal of the British Geomorphological Research Group*, 31(10), 1257-1279.
92. Beyeler, J. D., & Sklar, L. S. (2010, December). Bedrock resistance to fluvial erosion: The importance of rock tensile strength, crystal grain size and porosity in scaling from the laboratory to the field. In *AGU Fall Meeting Abstracts* (Vol. 2010, pp. EP41D-0740).
93. Lamb, M. P., Finnegan, N. J., Scheingross, J. S., & Sklar, L. S. (2015). New insights into the mechanics of fluvial bedrock erosion through flume experiments and theory. *Geomorphology*, 244, 33-55.
94. Sklar, L. S., & Dietrich, W. E. (2001). Sediment and rock strength controls on river incision into bedrock. *Geology*, 29(12), 1087-1090.
95. Moses, C., Robinson, D., & Barlow, J. (2014). Methods for measuring rock surface weathering and erosion: A critical review. *Earth-Science Reviews*, 135, 141-161.
96. Boumaiza, L., Saeidi, A., & Quirion, M. (2021). A method to determine the relative importance of geological parameters that control the hydraulic erodibility of rock. *Quarterly Journal of Engineering Geology and Hydrogeology*, 54(4), qjeh2020-154.
97. Selby, M. J. (1993). *Hillslope Materials* (p. 451). Oxford: Oxford university press.
98. Goudie, A. S. (2006). The Schmidt Hammer in geomorphological research. *Progress in Physical Geography*, 30(6), 703-718.
99. Giardino, J. R., & Lee, A. A. (2011). *Rates of channel migration on the Brazos River*. Yangling: Department of Geology & Geophysics, Texas A & M University.
100. Keller, E. A., & Pinter, N. (1996). *Active tectonics* (Vol. 338). Upper Saddle River, NJ: Prentice Hall.
101. Burnett, A. W. (1982). *Alluvial stream response to neotectonics in the lower Mississippi Valley* (Doctoral dissertation, Colorado State University).
102. Marín-Lechado, C., Galindo-Zaldívar, J., Gil, A. J., Borque, M. J., De Lacy, M. C., Pedrera, A., ... & de Galdeano-Equiza, C. S. (2010). Levelling profiles and a GPS network to monitor

- the active folding and faulting deformation in the Campo de Dalias (Betic Cordillera, Southeastern Spain). *Sensors*, 10(4), 3504-3518.
103. Tatar, M., Hatzfeld, D., Martinod, J., Walpersdorf, A., Ghafori-Ashtiany, M., & Chéry, J. (2002). The present-day deformation of the central Zagros from GPS measurements (DOI 10.1029/2002GL015427). *Geophysical research letters*, 29(19), 33-33.
104. Serpelloni, E., Faccenna, C., Spada, G., Dong, D., & Williams, S. D. (2013). Vertical GPS ground motion rates in the Euro-Mediterranean region: New evidence of velocity gradients at different spatial scales along the Nubia-Eurasia plate boundary. *Journal of Geophysical Research: Solid Earth*, 118(11), 6003-6024.
105. Rockwell, T. K., Keller, E. A., & Dembroff, G. R. (1988). Quaternary rate of folding of the Ventura Avenue anticline, western Transverse Ranges, southern California. *Geological Society of America Bulletin*, 100(6), 850-858.
106. Reyss, J. L., Pirazzoli, P. A., Haghypour, A., Hatte, C., & Fontugne, M. (1999). Quaternary marine terraces and tectonic uplift rates on the south coast of Iran. *Geological Society, London, Special Publications*, 146(1), 225-237.
107. Lees, G. M., & Falcon, N. L. (1952). The geographical history of the Mesopotamian plains. *The Geographical Journal*, 118(1), 24-39.
108. Soleimany, B., Poblet, J., Bulnes, M., & Sàbat, F. (2011). Fold amplification history unravelled from growth strata: the Dorood anticline, NW Persian Gulf. *Journal of the Geological Society*, 168(1), 219-234.
109. Khuzestan Water and Power Authority (KWPA) *Khuzestan Watersheds*. 2003. KWPA: Ahvaz, Iran.
110. Khuzestan Water and Power Authority (KWPA). *The Khuzistan Water and Power Authority*. Unpublished Résumé of the KWPA and Dams in Khuzestan; KWPA: Ahvaz, Iran, 2010; p. 11.
111. UN-ESCWA and BGR (United Nations Economic and Social Commission for Western Asia; Bundesanstalt für Geowissenschaften und Rohstoffe). *Chapter 5 - Shatt al Arab, Karkheh and Karun Rivers. 2013*. Inventory of Shared Water Resources in Western Asia: Beirut, Lebanon.
112. Kirkby, M. J. (1977). Land and water resources of the Deh Luran and Khuzistan plains. *Studies in the archaeological history of the Deh Luran Plain: the excavation of Chagha Sefid*, 251-288.
113. Verkinderen, P. (2015). Waterways of Iraq and Iran in the early Islamic period: changing rivers and landscapes of the Mesopotamian plain. (*No Title*).
114. Barry, R. G., & Chorley, R. J. (2009). *Atmosphere, weather and climate*. Routledge.
115. Kotteck, M., Grieser, J., Beck, C., Rudolf, B., & Rubel, F. (2006). *World Map of the Köppen-Geiger climate classification updated*, *Meteorol. Z.*, 15, 259–263.
116. Alijani, B. (2008). Effect of the Zagros Mountains on the spatial distribution of precipitation. *Journal of mountain science*, 5(3), 218-231.
117. Djmalali, M., Akhani, H., Andrieu-Ponel, V., Braconnot, P., Brewer, S., de Beaulieu, J. L., ... & Stevens, L. (2010). Indian Summer Monsoon variations could have affected the early-Holocene woodland expansion in the Near East. *The Holocene*, 20(5), 813-820.
118. Falcon, N. L. (1974). Southern Iran: Zagros Mountains. *Geological Society, London, Special Publications*, 4(1), 199-211.
119. Haynes, S. J., & McQuillan, H. (1974). Evolution of the Zagros suture zone, southern Iran. *Geological Society of America Bulletin*, 85(5), 739-744.
120. Alavi, M. (1994). Tectonics of the Zagros orogenic belt of Iran: new data and interpretations. *Tectonophysics*, 229(3-4), 211-238.
121. Berberian, M. (1995). Master “blind” thrust faults hidden under the Zagros folds: active basement tectonics and surface morphotectonics. *Tectonophysics*, 241(3-4), 193-224.
122. Jackson, J., Haines, J., & Holt, W. (1995). The accommodation of Arabia-Eurasia plate convergence in Iran. *Journal of Geophysical Research: Solid Earth*, 100(B8), 15205-15219.
123. Edgell, H. S. (1996). Salt tectonism in the Persian Gulf basin. *Geological Society, London, Special Publications*, 100(1), 129-151.
124. Hessami, K., Koyi, H. A., Talbot, C. J., Tabasi, H., & Shabanian, E. (2001). Progressive unconformities within an evolving foreland fold-thrust belt, Zagros Mountains. *Journal of the Geological Society*, 158(6), 969-981.
125. Hatzfeld, D., Authemayou, C., van Der Beek, P., Bellier, O., Lavé, J., Oveisi, B., ... & Yamini-Fard, F. (2010). The kinematics of the Zagros mountains (Iran).
126. Sella, G. F., Dixon, T. H., & Mao, A. (2002). REVEL: A model for recent plate velocities from space geodesy. *Journal of Geophysical Research: Solid Earth*, 107(B4), ETG-11.
127. Blanc, E. P., Allen, M. B., Inger, S., & Hassani, H. (2003). Structural styles in the Zagros simple folded zone, Iran. *Journal of the Geological Society*, 160(3), 401-412.
128. Allen, M., Jackson, J., & Walker, R. (2004). Late Cenozoic reorganization of the Arabia-Eurasia collision and the comparison of short-term and long-term deformation rates. *Tectonics*, 23(2).
129. Allen, M. B., Saville, C., Blanc, E. J. P., Talebian, M., & Nissen, E. (2013). Orogenic plateau growth: Expansion of the Turkish-Iranian Plateau across the Zagros fold-and-thrust belt. *Tectonics*, 32(2), 171-190.
130. Soleimany, B., & Sàbat, F. (2010). Style and age of deformation in the NW Persian Gulf. *Petroleum Geoscience*, 16(1), 31-39.
131. Heyvaert, V. M. A., & Walstra, J. (2016). The role of long-term human impact on avulsion and fan development. *Earth Surface Processes and Landforms*, 41(14), 2137-2152.
132. Heyvaert, V. M., Walstra, J., Verkinderen, P., Weerts, H. J., & Ooghe, B. (2012). The role of human interference on the channel shifting of the Karkheh River in the Lower Khuzestan plain (Mesopotamia, SW Iran). *Quaternary International*, 251, 52-63.
133. Upton, G., & Cook, I. (1996). *Understanding statistics*. Oxford University Press.
134. Salkind, N. J., & Frey, B. B. (2019). *Statistics for people who*

---

(think they) hate statistics. Sage Publications.

135. Li, F., Shi, X., Charreau, J., Cheng, X., Yang, R., Chen, H., ... & Wang, J. (2024). Geomorphic expression of transverse drainages across the Tugerming anticline, southern Tian Shan: Implications for the river-fold interaction in the foreland. *Journal of Structural Geology*, *180*, 105081.
136. Bullard, T. F., & Lettis, W. R. (1993). Quaternary fold deformation associated with blind thrust faulting, Los Angeles Basin, California. *Journal of Geophysical Research: Solid Earth*, *98*(B5), 8349-8369.
137. Hubbard, J., Shaw, J. H., Dolan, J., Pratt, T. L., McAuliffe, L., & Rockwell, T. K. (2014). Structure and seismic hazard of the Ventura Avenue anticline and Ventura fault, California: Prospect for large, multisegment ruptures in the western Transverse Ranges. *Bulletin of the Seismological Society of America*, *104*(3), 1070-1087.
138. Keller, E. A., Zepeda, R. L., Rockwell, T. K., Ku, T. L., & Dinklage, W. S. (1998). Active tectonics at Wheeler ridge, southern San Joaquin valley, California. *Geological Society of America Bulletin*, *110*(3), 298-310.
139. Keller, E. A., Gurrola, L., & Tierney, T. E. (1999). Geomorphic criteria to determine direction of lateral propagation of reverse faulting and folding. *Geology*, *27*(6), 515-518.
140. Gao, L., He, C., Rao, G., Yang, C. J., Yuan, X., Lai, J., ... & Wu, L. (2023). Numerical examination of the geomorphic indicators for lateral fold growth. *Geomorphology*, *432*, 108702.
141. Hurtrez, J. E., Lucazeau, F., Lavé, J., & Avouac, J. P. (1999). Investigation of the relationships between basin morphology, tectonic uplift, and denudation from the study of an active fold belt in the Siwalik Hills, central Nepal. *Journal of Geophysical Research: Solid Earth*, *104*(B6), 12779-12796.
142. Yanites, B. J., Tucker, G. E., Mueller, K. J., Chen, Y. G., Wilcox, T., Huang, S. Y., & Shi, K. W. (2010). Incision and channel morphology across active structures along the Peikang River, central Taiwan: Implications for the importance of channel width. *Bulletin*, *122*(7-8), 1192-1208.
143. Montgomery, D. R., & Stolar, D. B. (2006). Reconsidering Himalayan river anticlines. *Geomorphology*, *82*(1-2), 4-15.
144. Simpson, G. (2004). Role of river incision in enhancing deformation. *Geology*, *32*(4), 341-344.
145. Babault, J., Van Den Driessche, J., & Teixell, A. (2012). Longitudinal to transverse drainage network evolution in the High Atlas (Morocco): The role of tectonics. *Tectonics*, *31*(4).

## APPENDIX A

### A. Results of the New Scheme for the Rivers Karun, Dez and Karkheh

#### A.1. Short Description of the rivers Karun, Dez and Karkheh

##### A.1.1. River Karun (Iran)

*Length:* 890 km (from source to the Persian Gulf)

*Drainage Basin Area:* 45,230 km<sup>2</sup>

*Mean Annual Water Discharge:* 575 m<sup>3</sup>s<sup>-1</sup> (at Ahvaz in the Khuzestan Plains) [14,109]

*Seasonality of Discharge:* Maximum in April (c. 850 m<sup>3</sup>s<sup>-1</sup>, or more than 2,000 m<sup>3</sup>s<sup>-1</sup> prior to major dam construction); Minimum in October (c. 280 m<sup>3</sup>s<sup>-1</sup>) (at Ahvaz in the Khuzestan Plains).

*Major Direct Human Impacts on River:* Earliest major reservoir dam (constructed 1969–1976): Karun 1 or Shahid Abbaspour Dam at 32°03'N 49°36'E. Major dam at furthest downstream location: Lower Gotvand Dam at 32°17'N 48°50'E. Total of about 7 large reservoir dams [110,111].

*Short Description of River Course:* Source of Ab-e Kurang in central/eastern Zagros on slopes of Zardeh Kuh, elevation c. 4,200 m – very winding, roughly west and north-west course through Zagros Mountains, often in accordance with general NW-SE structural grain and folding, esp. large NW-SE Mungasht Anticline – generally west course across Zagros foothills – generally south and south-west course from Gotvand onwards across Upper Khuzestan Plains, with bifurcation at Shushtar into River Shuteyt (larger branch) to the west and River Gargar to the east, which re-unite at Band-e Qir in vicinity of confluence with River Dez – generally south-west course from Ahvaz across Lower Khuzestan Plains – joins Tigris-Euphrates-Karun delta at Khorramshahr, as south-east course of channels and distributaries flowing into Persian Gulf [14,36,112,113].

*Short Description of Climate: Warm steppic climate. Central Zagros* – various climates (mainly “sub-alpine”, “mountain forest steppe” and “xerophilous oak woodland”, annual precipitation c. 300 mm–1,000 mm or more); snowy winter, mild & rainy spring, dry summer/autumn; CSa, BSk, BSh (Köppen-Geiger Climate Classification) – Shahr-e Kord (32°20'N 50°52'E, elevation 2,070 m): mean daily Jan temp -2°C, mean daily July temp 24°C, mean annual precipitation 330 mm. *Zagros foothills and Upper Khuzestan Plains* – “pistachio-almond scrubs” and “semi-arid steppe”; BSh – Izeh (31°49'N 49°52'E, elevation 824 m): mean daily Jan temp 8°C, mean daily July temp 33°C, mean annual precipitation 383 mm. *Lower Khuzestan Plains* – “arid desert steppe”; limited winter & spring precipitation, long & very hot summer drought; BWh – Ahvaz (32°19'N 48°40'E, elevation 21 m): mean daily Jan temp 12°C, mean daily July temp 37°C, mean annual precipitation 209 mm [14,15,114–117].

*Short Description of Structural Geology: Foreland basin tectonic*

*setting.* Convergence of Arabian Plate towards Eurasian Plate producing four NW-SE trending regional structural zones (from Zagros orogen in north-east to foreland basin in south-west): Sanandaj-Sirjan (or metamorphic) Zone (S-SZ); Imbricated Zone (IZ); Simple Folded Zone (SFZ) (including Dezful Embayment); Mesopotamian-Persian Gulf Foreland Basin (FB) – initially (Jurassic/Cretaceous onwards) oceanic subduction of Arabian Plate beneath Eurasian Plate, then transition (in Oligocene/Early Miocene) to continent-continent collision – ongoing plate convergence in approx. S-N direction at c. 16–22 mm yr<sup>-1</sup> (c. 18 mm yr<sup>-1</sup> in Dezful Embayment where River Karun flows), producing mainly NW-SE trending thrust faults and folds. Earth surface movements in Khuzestan Plains and Zagros mainly by aseismic folding & faulting, and stable creep (probably due to lubricated décollements on evaporite layers) – earthquakes only account for small part of deformation. From Pliocene (c. 5 Ma) onwards deformation migrated away from orogen in north-east towards areas of thinner crust, producing successions of mainly NW-SE oriented thrust faults and associated NW-SE oriented detachment folds and fault bend folds. NW-SE oriented folds generally younger and less developed towards the south-west, dying out in vicinity of Zagros Deformation Front (ZDF) (NW-SE oriented line c. 30 km south-west of demarcation between Upper and Lower Khuzestan Plains). Folds are mainly asymmetric anticlines at or near ground surface – steeply dipping fore-limb to south-west and gently dipping back-limb to north-east. Typical fold lithostratigraphy in lowland south-west Iran: Quaternary deposits (c. 1 Ma–Present; unconsolidated alluvial sands, muds, gravels, and marls) – Middle Pliocene to Pleistocene Bakhtyari Formation (c. 3–1 Ma; well-consolidated conglomerates, sandstones, and mudstones) – Middle Miocene to Middle Pliocene Agha Jari Formation (c. 10–3 Ma; sandstones, marls, and mudstones) – Middle Miocene Mishan Formation (c. 16–10 Ma; marls, limestones, and sandstones) – Early Miocene Gachsaran Formation (c. 23–16 Ma; anhydrite and salt, limestones, marls, and shales). South-west of ZDF in FB are very slowly propagating, mainly N-S oriented folds, uplifts and lineaments. Some structural lineaments throughout lowland south-west Iran, with prominent c. 110 km long “concealed fault/deep-seated lineament” oriented E-W at about 31°47'N. Vertical Earth surface movements poorly known: Regional uplift to north-east of ZDF at c. 1 mm yr<sup>-1</sup> in central Zagros; regional subsidence to south-west of ZDF – fold uplift rates vary from about 0.01/0.024 mm yr<sup>-1</sup> in FB in Persian Gulf, to about 0.1–0.8 mm yr<sup>-1</sup> approx 20 – 60 km NE of the ZDF, to about 0.2 – 2.3 mm yr<sup>-1</sup> approx 60 – 130 km NE of the ZDF in Dezful Embayment [14,21,35,65,66,70,90,87,88,108,118–130].

##### A.1.2. River Dez (Iran)

*Length:* 515 km (from source to confluence with River Karun)

*Drainage Basin Area:* 23,250 km<sup>2</sup>

*Mean Annual Water Discharge:* 230 m<sup>3</sup>s<sup>-1</sup> [14,109]

*Seasonality of Discharge:* Similar to River Karun – Maximum in April; Minimum in October

*Major Direct Human Impacts on River:* Earliest (and largest) major reservoir dam (constructed 1959–1962): Dez Dam at 32°36'N 48°28'E. Major dam at furthest downstream location:

---

Dez Diversion Dam at 32°22'N 48°23'E. Total of about 5 large reservoir dams [110].

*Short Description Of River Course:* Source of Kamand (or Marboreh) River on Central Iranian Plateau, elevation c. 2,700 m – at confluence at Dorud becomes River Sehzar – roughly south-west course for River Sehzar (and its main tributary, River Bakhtyari) through the Zagros Mountains, mostly in discordance with general NW-SE structural grain and folding – generally south-west course across the Zagros foothills as River Dez – generally south and south-east course from Dezfoul onwards across Upper Khuzestan Plains, until confluence with River Karun at Band-e Qir [14,36,112].

*Short Description of Climate:* Very similar to River Karun – *Warm steppic climate.*

*Short Description of Structural Geology:* Very similar to River Karun – *basin tectonic setting.*

### **A.1.3. River Karkheh (Iran)**

*Length:* 755 km (from source to the Huwayzah Marshes)

*Drainage Basin Area:* 50,770 km<sup>2</sup>

*Mean Annual Water Discharge:* 165 m<sup>3</sup>s<sup>-1</sup> [14,109]

*Seasonality of Discharge:* Similar to River Karun – Maximum in April; Minimum in October

*Major Direct Human Impacts on River:* Earliest major reservoir dam (constructed 1992–2001): Karkheh Dam at 32°29'N 48°08'E. Major dam at furthest downstream location (completed in 1957): Hamidiya Regulating Dam at 31°34'N 48°27'E. Total of about 3 large reservoir dams [110,111,131].

*Short Description Of River Course:* Source of Gamas Ab on Central Iranian Plateau, elevation c. 3,100 m – at confluence with Qara Su to east of Kermanshah becomes River Saidmarreh – roughly south-west course for River Saidmarreh (and its main tributary, River Kashgan) through the Zagros Mountains, mostly in discordance with general NW-SE structural grain and folding – generally south-east course along flank of large NW-SE Kabir Kuh

Anticline – generally south course across the Zagros foothills as River Karkheh – generally south and south-east course across Upper Khuzestan Plains – changes in vicinity of Hamidiya to south-west course and then north-west course of channels and distributaries flowing into Huwayzah Marshes [36,64,111,131,132].

*Short Description of Climate:* Very similar to River Karun – *Warm steppic climate.*

*Short Description of Structural Geology:* Very similar to River Karun – *Foreland basin tectonic setting.*

### **A.2. Geomorphological Characteristics for the Rivers Karun, Dez and Karkheh**

The geomorphology of the study area is complex and has been affected by tectonic processes over time. The results for the 13 geomorphological characteristics when applying the scheme to the rivers Karun, Dez and Karkheh interacting with folds in lowland south-west Iran are given in Tables 2–9.

### **A.3. Statistical Analysis of Geomorphological Characteristics for the Rivers Karun, Dez and Karkheh**

In tabulated form, the results for the 13 geomorphological characteristics can be readily subjected to statistical analyses for investigating fold-river interactions. For the results of the rivers Karun, Dez and Karkheh in Tables 2–9, mean values have been calculated for the categories of river incision across a fold and river diversion around a fold for each of the 13 geomorphological characteristics, and Analysis of Variance (ANOVA) has been applied between these two categories for each of the 13 characteristics [14]. The ANOVA findings are summarised in Tables 10 and 11, in which  $F = \text{Obtained } F \text{ value (mean sums of squares due to between-group differences/ mean sums of squares due to within-group differences)}$ ,  $F_{crit} = \text{Critical } F \text{ value needed to reject the null hypothesis}$ ,  $p\text{-value} = \text{Level of significance of } F \text{ value}$ . In Tables 10 and 11, bold text and a yellow shading is used to highlight statistical significance, that is where the  $F$  value exceeds  $F_{crit}$  and where the  $p\text{-value} \leq 0.05$  (equivalent to a 5 % significance level or a 95 % confidence level) [78,133,134].

Geomorphological characteristic		Location of river reach or depth of sediments/ rocks	Turkalaki Anticline, TKA <i>River Karun</i> Incision across fold		Shushtar Anticline, STA <i>River Karun</i> Incision across fold		Qal'eh Surkheh Anticline, QSA <i>River Karun (Shuteyt)</i> Incision across projection of fold	
1	Channel width (m), <i>w</i>	Upstream	93.54		205.21		161.77	
		Across fold axis	253.53		113.45		245.87	
		Downstream	347.17		161.77		191.51	
2	Channel-belt width (km), <i>cbw</i>	Upstream	0.275		4.298		0.730	
		Across fold axis	0.424		0.652		2.698	
		Downstream	2.896		0.730		2.927	
3	Floodplain width (km), <i>fpw</i>	Upstream	0.526		5.396		1.222	
		Across fold axis	0.935		1.173		5.638	
		Downstream	14.625		1.222		10.248	
4	Channel sinuosity (no units), <i>Sc</i>	Upstream	1.125		1.345		1.392	
		Across fold axis	1.074		1.329		1.168	
		Downstream	1.368		1.392		1.283	
5	Braiding index (no units), <i>BI</i>	Upstream	1.0		1.7		2.0	
		Across fold axis	1.1		1.0		2.0	
		Downstream	2.4		2.0		3.1	
6	General river course direction (compass bearing in degrees relative to true north & relative to the fold axis), RCD	Upstream	280	45	180	50	250	40
		Across fold axis	205	60	205	75	205	85
		Downstream	170	25	250	60	225	65
7	Distance from fold core to location of river crossing (km), C-RC		3.9		4.5		1.2	
8	Distance from fold core to river basin margin (km), C-BM		+3.9		+8.6		+3.6	
9	Width of geological structure at location of river crossing (km), Wgs		2.3		7.4		7.5	
10	Estimate of erosion resistance of surface sediments/rocks and deeper sediments/rocks in fold (no units, relative scale from 1 to 9)	ERs (surface)	6		5		4	
		ERd (deeper)	7		7		6	
11	Maximum channel bank migration rate (m yr <sup>-1</sup> ), RMax	Upstream	8.037		12.022		12.634	
		Across fold axis	6.532		7.579		23.443	
		Downstream	14.437		12.634		48.082	
12	Transverse topographic symmetry of floodplain at location of river crossing (no units, offset of channel-belt towards or away from fold core), TSF		0.061	Towards fold core	0.444	Towards fold core	0.313	Towards fold core
13	Estimate of fold total uplift rate (no units, relative scale from 0 to 9), TUR		4		5		4	

**Table 2: Results For 13 Geomorphological Characteristics in Fold-River Interactions for The Turkalaki, Shushtar And Qal'eh Surkheh Anticlines**

Geomorphological characteristic		Location of river reach or depth of sediments/ rocks	Sardarabad Anticline, SDA <i>River Karun (Shuteyt)</i> Diversions around nose of fold		Qal'eh Surkheh Anticline, QSA <i>River Gargar</i> Incision across projection of fold		Kupal Anticline, KUA <i>River Gargar</i> Incision across fold (Near to fold nose)	
1	Channel width (m), <i>w</i>	Upstream	181.85		35.36		58.35	
		Across fold axis	202.19		56.54		33.58	
		Downstream	174.12		81.69		205.95	
2	Channel-belt width (km), <i>cbw</i>	Upstream	1.857		0.082		1.125	
		Across fold axis	2.051		0.314		0.154	
		Downstream	3.433		0.203		0.862	
3	Floodplain width (km), <i>fpw</i>	Upstream	8.414		0.207		3.650	
		Across fold axis	17.603		0.415		2.347	
		Downstream	13.030		0.386		5.442	
4	Channel sinuosity (no units), <i>Sc</i>	Upstream	1.798		1.066		2.629	
		Across fold axis	1.647		1.164		1.259	
		Downstream	1.682		1.243		1.061	
5	Braiding index (no units), <i>BI</i>	Upstream	1.1		1.0		1.0	
		Across fold axis	1.1		1.0		1.0	
		Downstream	1.0		1.0		1.0	
6	General river course direction (compass bearing in degrees relative to true north & relative to the fold axis), RCD	Upstream	135	0	195	85	250	70
		Across fold axis	190	55	190	80	215	75
		Downstream	190	55	140	30	180	40
7	Distance from fold core to location of river crossing (km), C-RC		32.2		4.8		43.6	
8	Distance from fold core to river basin margin (km), C-BM		-25.7		-3.6		-16.0	
9	Width of geological structure at location of river crossing (km), <i>Wgs</i>		4.1		7.5		6.8	
10	Estimate of erosion resistance of surface sediments/rocks and deeper sediments/rocks in fold (no units, relative scale from 1 to 9)	ERs (surface)	4		4		3	
		ERd (deeper)	6		6		6	
11	Maximum channel bank migration rate (m yr <sup>-1</sup> ), RMax	Upstream	32.291		0.664		7.939	
		Across fold axis	17.233		1.300		0.779	
		Downstream	46.727		0		3.412	
12	Transverse topographic symmetry of floodplain at location of river crossing (no units, offset of channel-belt towards or away from fold core), TSF		0.424	Towards fold core	0.070	Away from fold core	0.490	Towards fold core
13	Estimate of fold total uplift rate (no units, relative scale from 0 to 9), TUR		4		4		4	

**Table 3: Results For 13 Geomorphological Characteristics in Fold-River Interactions for The Sardarabad, Qal'eh Surkheh And Kupal Anticlines**

Geomorphological characteristic		Location of river reach or depth of sediments/ rocks	Dezful Uplift, DZU <i>River Dez</i> Incision across the uplift		Sardarabad Anticline, SDA <i>River Dez</i> Incision across fold		Shahur Anticline, SHA <i>River Dez</i> Diversion around nose of fold	
1	<b>Channel width</b> (m), <i>w</i>	Upstream	58.94		144.35		160.00	
		Across fold axis	68.19		139.24		161.26	
		Downstream	115.03		224.92		232.85	
2	<b>Channel-belt width</b> (km), <i>cbw</i>	Upstream	0.512		2.211		5.284	
		Across fold axis	0.365		0.833		7.297	
		Downstream	2.608		6.119		5.605	
3	<b>Floodplain width</b> (km), <i>fpw</i>	Upstream	6.245		8.690		9.611	
		Across fold axis	0.390		0.916		15.708	
		Downstream	18.734		6.646		11.841	
4	<b>Channel sinuosity</b> (no units), <i>Sc</i>	Upstream	1.036		1.417		1.629	
		Across fold axis	1.104		1.120		1.792	
		Downstream	1.140		1.585		2.231	
5	<b>Braiding index</b> (no units), <i>BI</i>	Upstream	1.0		1.0		1.0	
		Across fold axis	1.9		1.2		1.0	
		Downstream	6.5		1.2		1.0	
6	<b>General river course direction</b> (compass bearing in degrees relative to true north & relative to the fold axis), RCD	Upstream	230	75	130	10	140	25
		Across fold axis	225	80	230	70	185	70
		Downstream	195	70	135	15	155	40
7	<b>Distance from fold core to location of river crossing</b> (km), C-RC		15.6		1.3		22.8	
8	<b>Distance from fold core to river basin margin</b> (km), C-BM		+10.4		+3.8		-20.7	
9	<b>Width of geological structure at location of river crossing</b> (km), Wgs		2.8		4.3		4.9	
10	<b>Estimate of erosion resistance of surface sediments/rocks and deeper sediments/rocks in fold</b> (no units, relative scale from 1 to 9)	ERs (surface)	5		4		5	
		ERd (deeper)	7		6		6	
11	<b>Maximum channel bank migration rate</b> (m yr <sup>-1</sup> ), RMax	Upstream	2.527		51.907		26.630	
		Across fold axis	7.891		7.510		8.998	
		Downstream	22.038		27.671		11.838	
12	<b>Transverse topographic symmetry of floodplain at location of river crossing</b> (no units, offset of channel-belt towards or away from fold core), TSF		0	Central	0.060	Away from fold core	0.323	Towards fold core
13	<b>Estimate of fold total uplift rate</b> (no units, relative scale from 0 to 9), TUR		4		4		6	

**Table 4: Results For 13 Geomorphological Characteristics in Fold-River Interactions for The Dezful Uplift, and the Sardarabad and Shahur Anticlines**

Geomorphological characteristic		Location of river reach or depth of sediments/ rocks	Ramin Oilfield Anticline, ROA <i>River Karun</i> Incision across emerging fold		Ahvaz Anticline, AHA <i>River Karun</i> Incision across fold		Ab-e Teymur Oilfield Anticline, AOA <i>River Karun</i> Incision across emerging fold	
1	Channel width (m), <i>w</i>	Upstream	124.52		295.84		268.98	
		Across fold axis	325.07		320.27		191.18	
		Downstream	336.81		180.85		256.77	
2	Channel-belt width (km), <i>cbw</i>	Upstream	2.529		3.257		5.484	
		Across fold axis	0.871		0.664		0.876	
		Downstream	4.761		2.060		0.978	
3	Floodplain width (km), <i>fpw</i>	Upstream	4.271		18.701		35.538	
		Across fold axis	17.335		3.422		43.438	
		Downstream	25.937		27.424		42.440	
4	Channel sinuosity (no units), <i>Sc</i>	Upstream	1.702		2.167		3.283	
		Across fold axis	1.010		1.047		1.858	
		Downstream	2.468		1.078		1.176	
5	Braiding index (no units), <i>BI</i>	Upstream	1.0		1.2		1.0	
		Across fold axis	1.0		1.2		1.1	
		Downstream	1.1		1.0		1.0	
6	General river course direction (compass bearing in degrees relative to true north & relative to the fold axis), RCD	Upstream	130	25	215	75	265	55
		Across fold axis	185	30	220	70	235	85
		Downstream	230	75	265	25	230	90
7	Distance from fold core to location of river crossing (km), C-RC		1.7		8.5		0.6	
8	Distance from fold core to river basin margin (km), C-BM		+18.0		+22.0		+15.0	
9	Width of geological structure at location of river crossing (km), Wgs		4.0		2.3		4.4	
10	Estimate of erosion resistance of surface sediments/rocks and deeper sediments/rocks in fold (no units, relative scale from 1 to 9)	ERs (surface)	3		4		3	
		ERd (deeper)	5		5		5	
11	Maximum channel bank migration rate (m yr <sup>-1</sup> ), RMax	Upstream	21.608		9.201		9.447	
		Across fold axis	4.744		5.750		10.948	
		Downstream	9.443		9.350		5.163	
12	Transverse topographic symmetry of floodplain at location of river crossing (no units, offset of channel-belt towards or away from fold core), TSF		0.243	Towards fold core	0.200	Towards fold core	0.495	Towards fold core
13	Estimate of fold total uplift rate (no units, relative scale from 0 to 9), TUR		3		3		2	

**Table 5: Results For 13 Geomorphological Characteristics in Fold-River Interactions for The Ramin Oilfield Anticline, Ahvaz Anticline, And Ab-E Teymur Oilfield Anticline**

Geomorphological characteristic		Location of river reach or depth of sediments/ rocks	Dorquain Oilfield Anticline, DOA <i>River Karun</i> Diversions around nose of emerging fold		Dezful Uplift, DZU <i>River Karkheh</i> Diversions around the uplift		Dal Parri Anticline, DPA <i>River Karkheh</i> Diversions around nose of fold	
1	Channel width (m), <i>w</i>	Upstream	268.49		63.32		204.88	
		Across fold axis	171.64		84.60		98.51	
		Downstream	181.56		85.49		80.20	
2	Channel-belt width (km), <i>cbw</i>	Upstream	1.972		1.039		2.189	
		Across fold axis	0.754		0.455		2.026	
		Downstream	1.060		0.526		2.709	
3	Floodplain width (km), <i>fpw</i>	Upstream	75.022		1.675		16.151	
		Across fold axis	131.424		1.151		16.716	
		Downstream	131.459		0.842		15.269	
4	Channel sinuosity (no units), <i>Sc</i>	Upstream	1.675		1.641		1.154	
		Across fold axis	1.088		1.375		1.569	
		Downstream	1.014		1.162		1.292	
5	Braiding index (no units), <i>BI</i>	Upstream	1.0		1.0		2.9	
		Across fold axis	1.0		1.0		2.0	
		Downstream	1.0		1.2		1.4	
6	General river course direction (compass bearing in degrees relative to true north & relative to the fold axis), RCD	Upstream	190	10	105	0	180	45
		Across fold axis	230	50	145	40	170	35
		Downstream	245	65	185	80	175	40
7	Distance from fold core to location of river crossing (km), C-RC		26.5		13.5		20.9	
8	Distance from fold core to river basin margin (km), C-BM		+43.0		-10.4		+18.4	
9	Width of geological structure at location of river crossing (km), <i>Wgs</i>		9.2		4.6		17.0	
10	Estimate of erosion resistance of surface sediments/rocks and deeper sediments/rocks in fold (no units, relative scale from 1 to 9)	ERs (surface)	3		5		4	
		ERd (deeper)	5		7		6	
11	Maximum channel bank migration rate (m yr <sup>-1</sup> ), RMax	Upstream	8.655		—		7.288	
		Across fold axis	5.240		5.170		19.271	
		Downstream	1.913		4.837		26.376	
12	Transverse topographic symmetry of floodplain at location of river crossing (no units, offset of channel-belt towards or away from fold core), TSF		0.160	Away from fold core	0.605	Towards fold core	0.300	Away from fold core
13	Estimate of fold total uplift rate (no units, relative scale from 0 to 9), TUR		2		4		4	

**Table 6: Results For 13 Geomorphological Characteristics in Fold-River Interactions for The Dorquain Oilfield Anticline, Dezful Uplift, And Dal Parri Anticline**

Geomorphological characteristic		Location of river reach or depth of sediments/rocks	Sardarabad Anticline, SDA <i>River Karkheh</i> Diversion around nose of fold		Abu Salibi Anticline, ASA <i>River Karkheh</i> Diversion around nose of fold		Shahur Anticline, SHA <i>River Karkheh</i> Diversion around nose of fold	
1	Channel width (m), <i>w</i>	Upstream	68.59		81.50		86.41	
		Across fold axis	97.57		86.41		96.07	
		Downstream	88.82		96.07		90.46	
2	Channel-belt width (km), <i>cbw</i>	Upstream	3.026		3.939		4.307	
		Across fold axis	3.010		4.307		4.571	
		Downstream	5.668		4.571		5.478	
3	Floodplain width (km), <i>fpw</i>	Upstream	22.111		8.959		9.819	
		Across fold axis	19.268		9.819		10.688	
		Downstream	10.214		10.688		7.090	
4	Channel sinuosity (no units), <i>Sc</i>	Upstream	1.297		1.246		1.510	
		Across fold axis	1.193		1.510		2.867	
		Downstream	1.730		2.867		1.251	
5	Braiding index (no units), <i>BI</i>	Upstream	1.8		1.2		1.1	
		Across fold axis	2.2		1.1		1.2	
		Downstream	1.3		1.2		1.0	
6	General river course direction (compass bearing in degrees relative to true north & relative to the fold axis), RCD	Upstream	200	85	135	10	205	75
		Across fold axis	165	50	205	80	160	60
		Downstream	170	55	160	35	180	80
7	Distance from fold core to location of river crossing (km), C-RC		37.4		38.5		17.6	
8	Distance from fold core to river basin margin (km), C-BM		-3.8		+16.9		+20.7	
9	Width of geological structure at location of river crossing (km), Wgs		4.6		4.1		5.3	
10	Estimate of erosion resistance of surface sediments/rocks and deeper sediments/rocks in fold (no units, relative scale from 1 to 9)	ERs (surface)	4		5		5	
		ERd (deeper)	6		6		6	
11	Maximum channel bank migration rate (m yr <sup>-1</sup> ), RMax	Upstream	26.657		43.728		42.412	
		Across fold axis	52.833		42.412		49.726	
		Downstream	46.705		49.726		30.869	
12	Transverse topographic symmetry of floodplain at location of river crossing (no units, offset of channel-belt towards or away from fold core), TSF		0.221	<i>Away from fold core</i>	0.512	<i>Towards fold core</i>	0.514	<i>Towards fold core</i>
13	Estimate of fold total uplift rate (no units, relative scale from 0 to 9), TUR		4		3		6	

**Table 7: Results For 13 Geomorphological Characteristics in Fold-River Interactions for The Sardarabad, Abu Salibi, And Shahur Anticlines**

Geomorphological characteristic		Location of river reach or depth of sediments/ rocks	Darreh-ye Viza Anticline, DVA <i>River Karkheh</i> Diversion around nose of fold		Abu ul-Gharib Anticline, AGA <i>River Karkheh</i> Diversion around nose of fold		Dasht-e Mishan Oilfield, DMO <i>River Karkheh</i> Diversion around nose of emerging fold	
1	Channel width (m), <i>w</i>	Upstream	92.20		126.50		105.85	
		Across fold axis	87.48		116.75		88.48	
		Downstream	126.50		105.85		107.58	
2	Channel-belt width (km), <i>cbw</i>	Upstream	4.047		2.857		1.722	
		Across fold axis	5.383		3.807		3.664	
		Downstream	2.857		1.722		1.424	
3	Floodplain width (km), <i>fpw</i>	Upstream	7.153		4.391		4.971	
		Across fold axis	14.074		4.210		11.147	
		Downstream	4.391		4.971		1.892	
4	Channel sinuosity (no units), <i>Sc</i>	Upstream	1.542		2.402		1.657	
		Across fold axis	2.280		1.299		1.300	
		Downstream	2.402		1.657		1.974	
5	Braiding index (no units), <i>BI</i>	Upstream	1.1		1.1		1.2	
		Across fold axis	1.1		1.4		1.0	
		Downstream	1.1		1.2		1.0	
6	General river course direction (compass bearing in degrees relative to true north & relative to the fold axis), RCD	Upstream	110	5	145	35	140	0
		Across fold axis	135	20	135	25	240	80
		Downstream	145	30	140	30	245	75
7	Distance from fold core to location of river crossing (km), C-RC		15.0		24.2		15.1	
8	Distance from fold core to river basin margin (km), C-BM		+17.2		-11.2		+11.4	
9	Width of geological structure at location of river crossing (km), Wgs		3.7		4.5		3.5	
10	Estimate of erosion resistance of surface sediments/rocks and deeper sediments/rocks in fold (no units, relative scale from 1 to 9)	ERs (surface)	5		5		3	
		ERd (deeper)	6		6		5	
11	Maximum channel bank migration rate (m yr <sup>-1</sup> ), RMax	Upstream	35.772		19.342		26.656	
		Across fold axis	18.382		33.334		20.105	
		Downstream	19.342		26.656		31.052	
12	Transverse topographic symmetry of floodplain at location of river crossing (no units, offset of channel-belt towards or away from fold core), TSF		0.232	Away from fold core	0.696	Towards fold core	0.163	Towards fold core
13	Estimate of fold total uplift rate (no units, relative scale from 0 to 9), TUR		4		4		3	

**Table 8: Results For 13 Geomorphological Characteristics in Fold-River Interactions for The Darreh-Ye Viza Anticline, Abu Ul-Gharib Anticline, And Dasht-E Mishan Oilfield**

Geomorphological characteristic		Location of river reach or depth of sediments/ rocks	Zeyn ul-Abbas Anticline, ZUA River Karkheh Incision across fold		Hamidiyyeh Anticline, HAA River Karkheh Incision across fold		Susangerd Oilfield, SUO River Karkheh Diversion around nose of emerging fold	
1	Channel width (m), <i>w</i>	Upstream	107.58		185.26		139.61	
		Across fold axis	191.56		159.35		99.81	
		Downstream	185.26		122.74		80.11	
2	Channel-belt width (km), <i>cbw</i>	Upstream	1.424		2.041		0.655	
		Across fold axis	0.949		1.344		0.439	
		Downstream	2.041		4.347		0.562	
3	Floodplain width (km), <i>fpw</i>	Upstream	1.892		4.305		36.589	
		Across fold axis	1.034		4.265		34.287	
		Downstream	4.305		25.132		36.817	
4	Channel sinuosity (no units), <i>Sc</i>	Upstream	1.974		1.779		1.036	
		Across fold axis	1.183		1.179		1.148	
		Downstream	1.779		1.212		1.057	
5	Braiding index (no units), <i>BI</i>	Upstream	1.0		1.2		1.1	
		Across fold axis	1.0		1.6		1.0	
		Downstream	1.2		1.0		1.1	
6	General river course direction (compass bearing in degrees relative to true north & relative to the fold axis), RCD	Upstream	245	55	155	30	315	15
		Across fold axis	210	90	215	90	295	35
		Downstream	155	35	255	50	310	20
7	Distance from fold core to location of river crossing (km), C-RC		1.8		7.2		22.7	
8	Distance from fold core to river basin margin (km), C-BM		+11.8		+14.4		+13.7	
9	Width of geological structure at location of river crossing (km), <i>Wgs</i>		2.5		3.7		5.5	
10	Estimate of erosion resistance of surface sediments/rocks and deeper sediments/rocks in fold (no units, relative scale from 1 to 9)	ERs (surface)	4		4		3	
		ERd (deeper)	5		5		5	
11	Maximum channel bank migration rate (m yr <sup>-1</sup> ), RMax	Upstream	31.052		5.610		2.814	
		Across fold axis	1.664		6.701		7.828	
		Downstream	5.610		9.317		11.281	
12	Transverse topographic symmetry of floodplain at location of river crossing (no units, offset of channel-belt towards or away from fold core), TSF		0.008	Central	0.057	Towards fold core	0.863	Away from fold core
13	Estimate of fold total uplift rate (no units, relative scale from 0 to 9), TUR		3		3		2	

**Table 9: Results for 13 Geomorphological Characteristics in Fold-River Interactions for Zeyn Ul-Abbas Anticline, Hamidiyyeh Anticline, And Susangerd Oilfield**

Geomorphological characteristic		Mean value for river incision across a fold	Mean value for river diversion around a fold	Analysis of Variance (ANOVA) between categories of river incision across a fold and river diversion around a fold		
				<i>F</i>	<i>F crit</i>	<i>p</i> -value
1	<b>Channel width (m), <i>w</i></b> Difference between river reach immediately upstream of fold and river reach across fold axis	29.844	-15.703	2.542	4.301	0.1251
	<b>Channel width (m), <i>w</i></b> River reach across fold axis	174.819	115.898	3.713	4.301	0.0670
	<b>Channel width (m), <i>w</i></b> Difference between river reach across fold axis and river reach immediately downstream of fold	26.053	4.903	0.741	4.301	0.3987
2	<b>Channel-belt width (km), <i>cbw</i></b> Difference between river reach immediately upstream of fold and river reach across fold axis	-1.152	0.406	<b>6.923</b>	4.301	<b>0.0153</b>
	<b>Channel-belt width (km), <i>cbw</i></b> River reach across fold axis	0.845	3.147	<b>12.947</b>	4.301	<b>0.0016</b>
	<b>Channel-belt width (km), <i>cbw</i></b> Difference between river reach across fold axis and river reach immediately downstream of fold	1.699	-0.179	<b>7.634</b>	4.301	<b>0.0113</b>
3	<b>Floodplain width (km), <i>fpw</i></b> Difference between river reach immediately upstream of fold and river reach across fold axis	-0.778	6.769	2.180	4.301	0.1540
	<b>Floodplain width (km), <i>fpw</i></b> River reach across fold axis	6.776	23.841	2.547	4.301	0.1248
	<b>Floodplain width (km), <i>fpw</i></b> Difference between river reach across fold axis and river reach immediately downstream of fold	8.436	-3.133	<b>17.099</b>	4.301	<b>0.0004</b>
4	<b>Channel sinuosity (no units), <i>Sc</i></b> Difference between river reach immediately upstream of fold and river reach across fold axis	-0.535	0.040	<b>5.605</b>	4.301	<b>0.0271</b>
	<b>Channel sinuosity (no units), <i>Sc</i></b> River reach across fold axis	1.208	1.589	<b>5.440</b>	4.301	<b>0.0292</b>
	<b>Channel sinuosity (no units), <i>Sc</i></b> Difference between river reach across fold axis and river reach immediately downstream of fold	0.191	0.104	0.118	4.301	0.7349
5	<b>Braiding index (no units), <i>BI</i></b> Difference between river reach immediately upstream of fold and river reach across fold axis	0.083	-0.042	0.810	4.301	0.3778
	<b>Braiding index (no units), <i>BI</i></b> River reach across fold axis	1.258	1.258	0.000	4.301	1.0000
	<b>Braiding index (no units), <i>BI</i></b> Difference between river reach across fold axis and river reach immediately downstream of fold	0.617	-0.133	3.365	4.301	0.0801

**Table 10: Analysis of Variance (Anova) Between River Incision Across A Fold and River Diversion Around a Fold, Applied to Geomorphological Characteristics nos. 1 to 5 In Fold-River Interactions for The Rivers Karun, Dez And Karkheh In Lowland South-West Iran**

Geomorphological characteristic		Mean value for river incision across a fold	Mean value for river diversion around a fold	Analysis of Variance (ANOVA) between categories of river incision across a fold and river diversion around a fold			
				F	F crit	p-value	
6	<b>General river course direction</b> (compass bearing in degrees), RCD Change in river course direction between river reach immediately upstream of fold and river reach across fold axis	39.583	41.250	0.022	4.301	0.8837	
	<b>General river course direction</b> (compass bearing in degrees), RCD River reach across fold axis	Relative to true north	211.667	187.917	2.679	4.301	0.1159
		Relative to the fold axis	74.167	50.000	<b>10.430</b>	4.301	<b>0.0039</b>
	<b>General river course direction</b> (compass bearing in degrees), RCD Change in river course direction between river reach across fold axis and river reach immediately downstream of fold	41.667	16.250	<b>11.260</b>	4.301	<b>0.0029</b>	
7	<b>Distance from fold core to location of river crossing</b> (km), C-RC	7.892	23.867	<b>14.175</b>	4.301	<b>0.0011</b>	
8	<b>Distance from fold core to river basin margin</b> (km), C-BM +ve values where fold core is within drainage basin of river interacting with fold, -ve values where fold core is outside of drainage basin of river interacting with fold	7.658	5.792	0.082	4.301	0.7775	
	<b>Distance from fold core to river basin margin</b> (km), C-BM All +ve values, both where fold core is within drainage basin and outside of drainage basin of river interacting with fold	10.925	17.758	4.085	4.301	0.0556	
9	<b>Width of geological structure at location of river crossing</b> (km), Wgs	4.625	5.917	1.064	4.301	0.3136	
10	<b>Estimate of erosion resistance of surface sediments/rocks and deeper sediments/rocks in fold</b> (no units, relative scale from 1 to 9)	ERs (surface)	4.083	4.250	0.214	4.301	0.6485
		ERd (deeper)	5.833	5.833	0.000	4.301	1.0000
11	<b>Maximum channel bank migration rate</b> (m yr <sup>-1</sup> ), RMax Difference between river reach immediately upstream of fold and river reach across fold axis	-7.317	0.283	1.478	4.325	0.2375	
	<b>Maximum channel bank migration rate</b> (m yr <sup>-1</sup> ), RMax River reach across fold axis	7.070	23.378	<b>9.706</b>	4.301	<b>0.0050</b>	
	<b>Maximum channel bank migration rate</b> (m yr <sup>-1</sup> ), RMax Difference between river reach across fold axis and river reach immediately downstream of fold	1.208	4.301	0.2837			
12	<b>Transverse topographic symmetry of floodplain at location of river crossing</b> (no units), TSF	0.203	0.418	<b>6.352</b>	4.301	<b>0.0195</b>	
13	<b>Estimate of fold total uplift rate</b> (no units, relative scale from 0 to 9), TUR	3.583	3.833	0.336	4.301	0.5683	

**Table 11: Analysis of Variance (Anova) Between River Incision Across A Fold and River Diversion Around a Fold, Applied to Geomorphological Characteristics Nos. 6 to 13 In Fold-River Interactions for The Rivers Karun, Dez And Karkkeh In Lowland South-West Iran**

---

## APPENDIX B

### B. Discussion of Results of the New Scheme for the Rivers Karun, Dez and Karkheh

#### *B.1. Geomorphological Characteristics with Statistical Significance for Discriminating Between River Incision and River Diversion for the Rivers Karun, Dez And Karkheh*

As can sometimes be the case in geomorphology, the values of the 13 geomorphological characteristics will, to a certain extent, vary according to where and how the observer selects to take the measurements. Thus, it is necessary to follow the directions given with the descriptions of each of the 13 characteristics, so that the measurements are standardised. This is especially the case with the subdivision into river reaches and the determination of the location of the fold core, where a greater degree of subjectivity is involved. Hence, it may be useful to include error estimates with the measurements of the geomorphological characteristics.

Considering this, and the natural variability and complexity of major rivers [9,42], it could be the case that none of the 13 geomorphological characteristics would show statistically significant differences between the categories of river incision across a fold and river diversion around a fold. Nevertheless, the Analysis of Variance (ANOVA) findings in Tables 10 and 11 show seven geomorphological characteristics with statistically significant differences at the 95 % confidence level ( $p$ -value  $\leq 0.05$ ) between river incision and river diversion for the rivers Karun, Dez and Karkheh interacting with folds in lowland south-west Iran: channel-belt width ( $cbw$ ), floodplain width ( $fpw$ ), channel sinuosity ( $Sc$ ), general river course direction (RCD), distance from fold core to location of river crossing (C-RC), maximum channel bank migration rate (RMax), and transverse topographic symmetry of floodplain (TSF) (geomorphological characteristics Nos. 2, 3, 4, 6, 7, 11 and 12).

Channel-belt width ( $cbw$ ) is significantly decreased for river incision across a fold compared with river diversion around a fold, for the river reach across the fold axis. Also, it is significantly decreased for river incision for the difference between the river reach immediately upstream of the fold and the river reach across the fold axis, and significantly increased for river incision for the difference between the river reach across the fold axis and the river reach immediately downstream of the fold. Channel-belt width is the only geomorphological characteristic to be statistically significantly different in all three of these scenarios. In cases of river diversion, channel-belt width at the location of the projection of the fold axis may have a wide range of values. By contrast, in cases of river incision, channel-belt width is always (100 % of cases) less than 2.7 km at the location of the fold axis. This implies that there is a narrowing of the channel-belt as a response of a major river when incising across a fold. A narrow channel-belt at the location of the fold axis is indicative of a reduction in the lateral migration of the river, as a mechanism to increase vertical incision of the river to keep pace with fold uplift. [14,28]. The general scenario is one of

broader channel-belts immediately upstream and downstream of the fold due to increased aggradation to maintain channel slopes across the fold, and narrow channel-belts across the fold due to increased erosion and incision to keep pace with fold uplift [33,47,48]. A narrow channel-belt is present in all cases of river incision, probably because a channel-belt is a relatively small feature that typically develops over time intervals of several decades or more [57,77]. Indeed, an average channel-belt width of 2.7 km or less may be a threshold for the rivers Karun, Dez and Karkheh in the Khuzestan Plains that needs to be maintained if a major river is incised across a fold in the long-term [14].

Floodplain width ( $fpw$ ) is significantly different for river incision across a fold compared with river diversion around a fold, though only as a significant increase for river incision for the difference between the river reach across the fold axis and the river reach immediately downstream of the fold. This is probably because, in cases of river incision across a fold, there is a tendency towards a reduction in the floodplain width as a river incises across a fold axis (though not to a statistically significant degree), and then a subsequent statistically significant increase in the floodplain width immediately downstream of the fold. In a manner similar to that for the channel-belt width characteristic, a narrow floodplain at the location of the fold axis may be indicative of a reduction in the lateral migration of the river to increase vertical incision of the river to keep pace with fold uplift. [14,28]. However, for the floodplain width characteristic this effect appears to be slight, and is only pronounced immediately downstream of the fold where there is sufficient space on the Khuzestan Plains for the floodplain to spread out and widen significantly. This may be because a floodplain is a relatively large feature that typically develops over time intervals of centuries [64]. Thus, in extensive, relatively flat areas, such as the Lower Khuzestan Plains, the streams and wetlands of the floodplain of a major river may extend far beyond the surface expression of a small fold and thus be largely unaffected by it.

Channel sinuosity ( $Sc$ ) is significantly decreased for river incision across a fold compared with river diversion around a fold, for the river reach across the fold axis. Also, it is significantly decreased for river incision for the difference between the river reach immediately upstream of the fold and the river reach across the fold axis. For the rivers Karun, Dez and Karkheh in the Khuzestan Plains, mean channel sinuosity decreased from 1.743 immediately upstream of the fold to 1.208 across the fold axis for river incision, whereas mean channel sinuosity increased very slightly 1.549 to 1.589 for river diversion for the same scenarios. This implies that there is a reduction in channel sinuosity, or a straightening of the river channel, as a response of a major river when encountering a fold and incising across it. A reduction in channel sinuosity at the location of the fold axis may be a mechanism to increase vertical incision of the river to keep pace with fold uplift [14,28,50,135]. If so, this mechanism will be time-limited, particularly because once incised meanders have formed (as is the case for river incision across the Shushtar Anticline), any subsequent changes to channel sinuosity will be inhibited. Interestingly, there is no statistically significant increase in channel sinuosity immediately downstream of a fold

---

(a mean increase of 0.191 for river incision, which is only slight and very similar to the mean increase of 0.104 for river diversion). This may be partly because reduced vertical incision immediately downstream of a fold may be promoted by other geomorphological changes, such as increases in floodplain width and braiding index. Further work with major rivers with braided channel patterns is needed to investigate this.

General river course direction relative to the fold axis (RCD) is significantly increased for river incision across a fold compared with river diversion around a fold, for the river reach across the fold axis. Also, for river incision across a fold, there is a significantly greater change in river course direction between the river reach across the fold axis and the river reach immediately downstream of the fold. This indicates that for the rivers Karun, Dez and Karkheh in the Khuzestan Plains, in cases of river incision there is a tendency for the river channel to become more orthogonal to the fold axis when crossing the fold axis (mean value  $74.167^\circ$ ) and then to revert to the “original” river course direction immediately downstream of the fold (mean value of change  $41.667^\circ$ ). This hypothesis is supported by data for cases of river incision showing a very similar change in river course direction immediately upstream of the fold (mean value of change  $39.583^\circ$ ) and immediately downstream of the fold (mean value of change  $41.667^\circ$ ). By contrast, in cases of river diversion around a fold, there is a tendency for the river channel to become more orthogonal to the fold axis when crossing the fold axis, though this is significantly less pronounced (mean value  $50.000^\circ$ ) and any reversion to its “original” river course direction immediately downstream of the fold is fairly slight (mean value of change  $16.250^\circ$ ). Changes in river course direction immediately upstream of the fold are very similar in cases of river incision and river diversion, since, as might be expected, the deflection of river course tends to be similar, be it a deflection to the location of the “water gap” or to the location of the nose of the fold. In cases of river incision across a fold, the change in general river course direction to become more orthogonal to the fold axis when crossing the fold axis may be a mechanism to increase the vertical incision of the river to keep pace with fold uplift [14,28].

Distance from fold core to location of river crossing (C-RC) is significantly decreased for river incision across a fold compared with river diversion around a fold. This difference is pronounced for the rivers Karun, Dez and Karkheh in the Khuzestan Plains, with a mean value of 7.892 km for cases of river incision compared with a mean value of 23.867 km for cases of river diversion. It is not unexpected that the distance from the fold core to the location of the river crossing should discriminate between the two categories of fold-river interactions, since river incision occurs between the fold core and the fold nose, and river diversion occurs beyond the fold nose. Indeed, in all but one case of river incision C-RC is less than 16 km (the exception of 43.6 km for the River Gargar incising across the Kupal Anticline is associated with pronounced human influences on the development of the River Gargar), whereas in all cases of river diversion the distance is greater than 13 km. Interestingly, there is a strong tendency for the river to incise across the fold at locations near to that of the fold core (8.5 km or less in 83 % of cases). Since

the folds in the Khuzestan Plains are relatively young folds, this suggests that river incision across a fold at, or near to, the fold core is initiated at a very early stage in fold development, probably when the fold is initially emerging on the ground surface [14].

Maximum channel bank migration rate (RMax) is significantly decreased for river incision across a fold compared with river diversion around a fold, for the river reach across the fold axis. This difference is pronounced for the rivers Karun, Dez and Karkheh in the Khuzestan Plains, with a mean value of  $7.070 \text{ m yr}^{-1}$  for cases of river incision across a fold compared with a mean value of  $23.378 \text{ myr}^{-1}$  for cases of river diversion around a fold. This implies that there is reduced migration of the river channel at the location of the fold axis, as a response of a major river when incising across a fold. Though this reduction in maximum channel bank migration rate is manifest in the data for cases of river incision (a mean difference of  $-7.317 \text{ m yr}^{-1}$  between reaches immediately upstream of the fold and across the fold axis, and a mean difference of  $6.860 \text{ m yr}^{-1}$  between reaches across the fold axis and immediately downstream of the fold), the changes are not statistically significant when compared with cases for river diversion. Hence, a reduction in maximum channel bank migration rate at the location of the fold axis may be a mechanism to increase vertical incision of the river to keep pace with fold uplift, albeit fairly slight [14,28,50].

Transverse topographic symmetry of floodplain at the location where the river channel thalweg crosses the fold axis (TSF) is significantly reduced for river incision across a fold compared with river diversion around a fold. For the rivers Karun, Dez and Karkheh in the Khuzestan Plains, there is a mean value of 0.203 for cases of river incision compared with a mean value of 0.418 for cases of river diversion. This indicates that with cases of river diversion, there is a tendency for the channel-belt to be located more towards the edge of the floodplain. Whilst there may be a variety of factors influencing this [28,59], it may not be primarily a response to ground tilting, since if ground tilting were the main factor, one might expect that most cases of river diversion would have TSF displaced away from the fold core, whereas for the rivers Karun, Dez and Karkheh for cases of river diversion they are roughly evenly spread (7 cases displaced towards the fold core, 5 cases displaced away from the fold core). Rather, it may be influenced more by other factors, such as when a river is diverted around a fold “nose”, the river may then incise near to the fold “nose”, resulting in a channel-belt relatively near to the edge of the floodplain. Also, when a river is diverted around a fold, the river channel may be more “mobile” (the river may be more subject to channel bank migration), resulting in a channel-belt that could be located anywhere within the floodplain, rather than tending to be near to the floodplain midline. As noted above, C-RC is significantly decreased and RMax is significantly decreased for river incision across a fold compared with river diversion around a fold, for the river reach across the fold axis. The differences in TSF between cases of river incision and river diversion may due to rivers incising across a fold tending to incise relatively near to the fold “core” and then being less “mobile” (less subject to channel bank migration), resulting in a channel-belt located relatively near to the midline of the floodplain. More data is needed from other major rivers in different environments to determine if this is the case.

## ***B.2. Geomorphological Characteristics with Differences Between River Incision and River Diversion That Are Not Statistically Significant for The Rivers Karun, Dez And Karkheh***

This leaves six geomorphological characteristics with no statistically significant differences at the 95 % confidence level ( $p$ -value  $\leq 0.05$ ) between river incision and river diversion for the rivers Karun, Dez and Karkheh interacting with folds in lowland south-west Iran: channel width ( $w$ ), braiding index ( $BI$ ), distance from fold core to river basin margin (C-BM), width of geological structure ( $Wgs$ ), estimate of erosion resistance of fold sediments/rocks (ERs, ERd), and estimate of fold total uplift rate (TUR) (geomorphological characteristics Nos. 1, 5, 8, 9, 10 and 13).

Channel width ( $w$ ) shows no statistically significant differences between cases of river incision across a fold and river diversion around a fold. The reason for this is uncertain. The conceptual model of Amos and Burbank [26] and the studies of Lavé and Avouac [51,52] in Nepal indicate that narrowing of the channel width is a key response in cases of river incision across a fold, yet, if anything, for the rivers Karun, Dez and Karkheh in the Khuzestan Plains the channel width for the river reach across the fold axis is broader in cases of river incision (mean value 174.819 m) than in cases of river diversion (mean value 115.898 m). Maybe the river channel is slightly broader, with more river islands, at the fold axis in cases of river incision, due to a tendency for the river bed to encounter more erosion resistant bedrock at the location of the fold axis and the associated high rates of uplift. More probably, channel width is so varied in major rivers, especially due to local irregularities, that any differences between river incision and river diversion are insignificant. More data from other major rivers across the globe, including upland rivers, is needed to investigate this.

Braiding index ( $BI$ ) shows no statistically significant differences between cases of river incision across a fold and river diversion around a fold, probably merely because there is only limited variation in the data. Most river reaches in the region have a braiding index ranging from 1.0 to 1.3, due to the preponderance of single-thread meandering and straight channel patterns for major rivers in the region. Data with greater variation from regions with mostly multi-thread braided channel patterns is needed.

For distance from fold core to river basin margin (C-BM), there is a strong tendency for the fold core to be located within the drainage basin of the river interacting with the fold for cases of river incision (83 % of cases have +ve values of C-BM), though this tendency is also present for cases of river diversion (58 % of cases have +ve values of C-BM). Hence, C-BM shows no statistically significant differences between cases of river incision across a fold and river diversion around a fold, though it is close to statistical significance ( $p$ -value 0.0556) when all measurements are expressed as +ve values, with a mean value of 10.925 km for cases of river incision

and 17.758 km for cases of river diversion. There may be a tendency for C-BM to be greater in cases of river diversion because of the timing of fold-river interactions; as the fold grows from the fold core it may actively divert both the river system and its basin margin, making the distance from the fold core to the river basin margin greater. If this were the case, then it would be expected that this difference in C-BM would reach statistical significance when more data from other major rivers is available.

Width of geological structure ( $Wgs$ ) shows no statistically significant differences between cases of river incision across a fold and river diversion around a fold. This may be because for the major rivers of the size of the rivers Karun, Dez and Karkheh in the Khuzestan Plains, fold widths of 2.3 km up to 7.5 km and 17.0 km are, in general, not wide enough to influence river responses. This may be found to be different when data from other major rivers in a variety of environments is available.

Estimate of erosion resistance of fold sediments/rocks (ERs for surface and ERd for deeper) shows no statistically significant differences between cases of river incision across a fold and river diversion around a fold, maybe because there is only limited variation in the data. In particular, at a local scale in the Khuzestan Plains, the folds all exhibit a very similar lithology, so a river will initially encounter a very similar surface erosion resistance, irrespective of the fold and how it interacts with it. The main difference at a local scale is between erosion resistance at the surface, ERs, and erosion resistance deeper, ERd, with deeper sediments and rocks only encountered after significant river incision has occurred. Hence, when data from more major rivers is available, a comparison of some form between ERd for river incision across a fold and ERs for river diversion around a fold may be useful.

Estimate of fold total uplift rate (TUR) shows no statistically significant differences between cases of river incision across a fold and river diversion around a fold. As with the geomorphological characteristic of erosion resistance of fold sediments/rocks, this may be because there is only limited variation in the data. In particular, at a local scale in the Khuzestan Plains, folds will have a very similar TUR due being within one of the NW-SE trending approximate zones of Earth surface movements in the region: A (subsidence), B (minimal uplift), C (uplift of approx 0.1 – 0.8 mm yr<sup>-1</sup>), or D (uplift of approx 0.2 – 2.3 mm yr<sup>-1</sup>), as shown in Figure 2 [14,21]). There may be a few folds that are “outliers” for these zones (such as the Shahur Anticline in zone C, which may have a relatively high TUR of about  $2.03 \pm 0.10$  mm yr<sup>-1</sup> [14]), but these may not be numerous enough to elucidate any significant differences in river responses, should they exist. More data is needed from regions which have folds with notably different uplift rates, particularly at the local scale, such as may be the case in coastal southern California, USA [96,136,137].

*Copyright: ©2025 Daniel R. Parsons, et al. This is an open-access article distributed under the terms of the Creative Commons Attribution License, which permits unrestricted use, distribution, and reproduction in any medium, provided the original author and source are credited.*